Vol. 1 June, 1956 No. 6

MINERALOGICAL JOURNAL

CONTENTS

Vivianite from Himeshima, Ooita Prefecture, Japan .....
.....H. Minato, K. Kinoshita and Y. Okamoto ...337
Magnesium-rich Chlorite from the Wanibuchi Mine, Shimane Prefecture..... T. Sakamoto and T. Sudo...348
Effects of Constituent Cations on the Refractive Indices of Orthopyroxenes..... F. Hori...359
Optical Properties and Unit Cell Dimensions of Cordierite and Indialite..... T. Iiyama...372

Short Communications

Chlorite from the Hitachi Mine, Ibaragi Prefecture.....
.....H. Sato and T. Sudo...395
Index to Volume 1.....398
Title-page and Contents

The Mineralogical Society of Japan
Department of Geology and Mineralogy, Faculty of Science,
Hokkaido University, Sapporo, Japan

MINERALOGICAL JOURNAL

published by

The Mineralogical Society of Japan

EDITORIAL BOARD

Zyunpei HARADA, *Hokkaido University;* Teiichi ITO, *University of Tokyo;* (Chief) Nobuo KATAYAMA, *University of Tokyo;* Keiichi OMORI, *Tohoku University;* Ryôiti KIRIYAMA, *University of Osaka;* Seitaro TSUBOI, *University of Tokyo;* Takeo WATANABE, *University of Tokyo;* Toyofumi YOSHIMURA, *Kyushu University.*

Instructions to Contributors

Manuscripts of articles should be submitted to the executive editor, Nobuo Katayama, at the College of General Education, University of Tokyo, Komaba, Meguro-ku, Tokyo. The manuscript should be type-written with double space lines, and not exceed 20 sheets of normal type-writing paper. References of literature should be in accordance with the forms used in the pages of this journal.

Plates and figures should be capable of reduction to not more than 10 by 15 centimetres. Line drawings should be in black India ink on white drawing board, tracing paper, or coordinate paper printed in blue. Photographs should be positive glossy prints.

Two referees chosen by the Editorial Board read the manuscript of article submitted before it is accepted for publication.

Thirty reprints without cover will be furnished to the author free of cost and without previous notice from him. Additional reprints will be furnished at cost when ordered.

The price of the journal to subscribers in Japan is 250 yen for a single copy (including postage), and to subscribers in other countries $ 1.00 (including postage).

Printed in Japan

MINERALOGICAL JOURNAL, VOL. 1, No. 6, pp. 337 347, JUNE, 1956

VIVIANITE FROM HIMESHIMA, OOITA PREFECTURE, JAPAN*

(Studies on Vivianite from Japan, Rept. 1)

HIDEO MINATO,

Institute of Earth Science, College of General Education, University of Tokyo

KAMEKI KINOSHITA,

Institute of Economic Geology, Faculty of Engineering, Kyushu University

and YOHACHIRO OKAMOTO

Institute of Geology and Mineralogy, Faculty of Science, Kyushu University

ABSTRACT

Vivianite nodules 1~8 cm. in diameter, some of them taking the shape of tree-trunk or mammal bone, have been found in gravels and mudstone bed at the beach Subana in the Island of Himeshima, Ooita Prefecture, Japan. They are composed of radial aggregates of foliated vivianite crystals. The specimens collected from the gravels are covered with brown film of limonite. The observation on the fresh vivianite from Himeshima follows; colour: yellowish or deep blue, streak: blue, hardness: 1.5~2, sp. gr.: 2.66 at 17°C., cleavage: (010) easy, luster: vitreous, indices of refraction: $\alpha=1.587$, $\beta=1.607$ and $\gamma=1.631$, 2V large, pleochroism: X blue, Y colourless or yellowish and Z yellowish, optical orientations: X//b, Z$\wedge$c about 27°. Small but good crystals of vivianite are found on the wall of druses. They have short prismatic habit with monoclinic symmetry. Forms: *b* (010), *m* (110), *w* ($\bar{2}$01), *T* (103), *d* (801), *x* (221) and *V* (441). The result of chemical analysis of a nodular specimen follows, P_2O_5 24.43, Al_2O_3 2.49, Fe_2O_3 6.84, FeO 30.04, MnO 0.24, MgO 0.28, CaO 0.06, Na_2O tr., K_2O tr., TiO_2 tr., SiO_2 non., SO_3 non., insol. 10.36, $H_2O(+)$ 13.05, $H_2O(-)$ 12.65, total 100.44%, and that of a specimen in tree trunk shape follows, P_2O_5 26.84, Al_2O_3 0.59, Fe_2O_3 14.00, FeO 29.30, MnO tr., MgO 0.10, CaO 0.12, SiO_2 0.42, insol. 0.06, $H_2O(+)$ 16.11,

* Preliminary reports of this work were read at the meetings of the Geological Society of Japan in March 1952 and in March 1955.

$H_2O(-)$ 12.35, total 99.89%. In the nodular sample, some clay inclusions are observed under the microscope. The main features of X-ray powder diagram of the tree-trunk-shaped specimen agrees with that of the well crystallized vivianite from the Ashio mine, Tochigi Prefecture, Japan.

Introduction

Though blue-coloured earthy or powdery vivianite is found from various sedimentary beds, compact vivianite nodules[3] rarely occur in Japan. Recently, vivianites in the shape of compact nodules or pseudomorphous after tree trunks or bones of mammals were found at a sea shore in the Island of Himeshima, Ooita Prefecture.[4] Its occurrence was studied by the present writers and its mineralogical investigations were carried out by one of the writers (H. M.).

Occurrence

The locality of the vivianite is Subana, Himeshima-mura, Higashi-Kunizaki-gun, Ooita Prefecture,* in the southwestern portion of the Island of Himeshima, which is situated at the western fringe of Setonaikai, and accessible from Port Imi, Kunizaki Peninsula or from Beppu by ferry-steamer. Himeshima is four kilometers from east to west and one kilometer from north to south. The eastern and western parts of the Island are built up of volcanic hills which are composed of hornblende andesite, biotite-bearing hornblende andesite and their clastic materials, and its

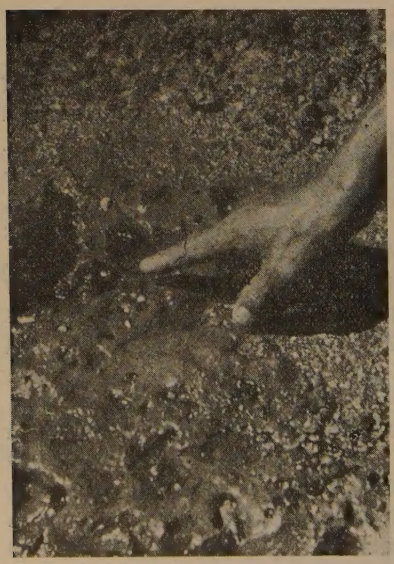

Fig. 1. Vivianite nodule in a mudstone bed in Himeshima.

* 大分県東国東郡姫島村ス鼻

Fig. 2. Vivianite nodule sticking on mudstone from Himeshima.
V: vivianite, M: mudstone. (×0.8)

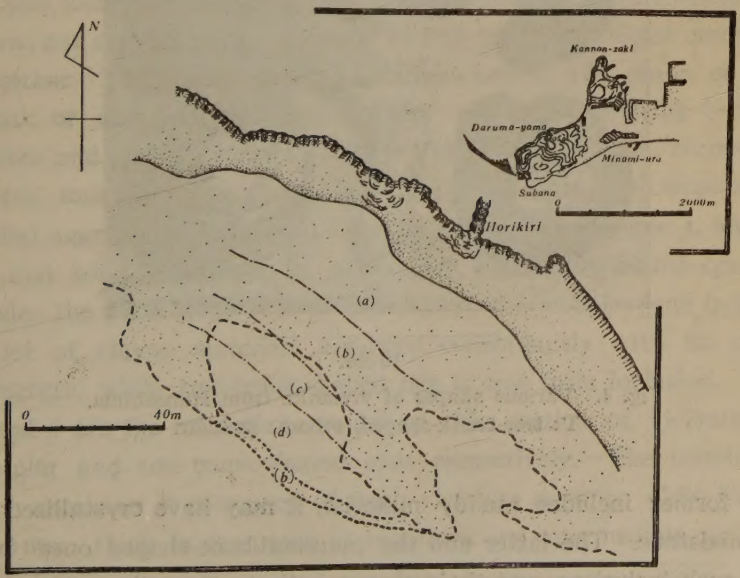

Fig. 3. Sketch map of the locality of vivianite in Himeshima.
Zone (a) and (d): without vivianite, zone (b): vivianite among gravels, and zone (c): vivianite in mudstone.

central part is of alluvial plane with their debris. The occurrence of the vivianite is of two types: one occurs among shore gravels and the other in mudstone bed below the sea level and is observable when the tide is neap.

A vivianite nodule in mudstone is illustrated in Fig. 1, and another nodule sticking on mudstone in Fig. 2. Such nodules were dug out from mudstone by marine erosion and intermingled with shore gravels, the surface of them being oxidized to limonite. The distribution of vivianite in Subana is sketched in a map as Fig. 3.

There are three types of vivianite in Subana, one is nodular and the others are in the shape of tree trunk or of mammal bone. The nodular and tree-trunk-shaped ones[1] are illustrated in Fig. 4. Since

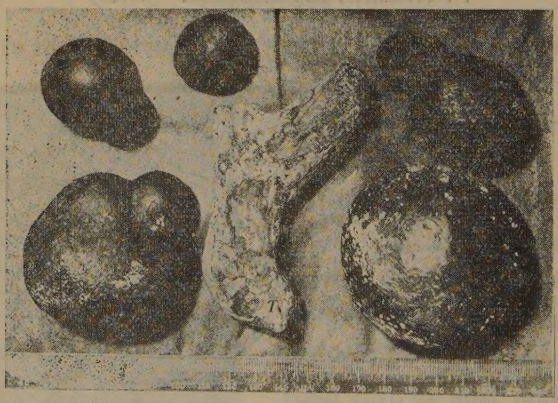

Fig. 4. Various shapes of vivianite from Himeshima.
T: tree-trunk-shaped, others: nodular.

the former includes muddy material, it may have crystallized out in mudstone. The latter and the mammal-bone-shaped ones[5] have not such inclusions, and their shapes indicate that they may have been formed by replacement of tree or bone with vivianite.

Part of the phosphorous in these vivianite may have been derived

from mammal bodies, for some mammal fossils* were collected from the same locality as of vivianite. However, judging from the amount of vivianite and fossils in Subana, a majority of the phosphorous in vivianite seems to have been derived not from mammal but from mudstone, which contains a small amount of phosphorous. The result of chemical analysis of the mudstone free from vivianite is as follows: SiO_2 51.81, TiO_2 0.40, Al_2O_3 17.54, Fe_2O_3 4.44, MnO tr., MgO 0.97, CaO 1.07, Na_2O 1.68, K_2O 1.14, P_2O_5 0.23, H_2O (+) 13.02, H_2O (−) 7.22, total 99.52% (analysed by H. Minato, 1954).

General characters, optical properties and the observations under the microscope

The fresh vivianite from mudstone bed has blue colour and rough surface, but the one collected from among shore gravels is covered by brown limonite film with smooth surface. Most of the vivianites of this locality show spherulitic nodular form with diameters 1~8 cm., and some specimen consists of two or three nodules combined together. There are also a few vivianites in the shape of tree trunk or mammal bone, the largest of the former being 1~5 cm. across and 50 cm. long, and that of the latter, 5~15 cm. across and 60 cm. long. Nodular and tree-trunk-shaped ones are composed of radial aggregates of foliated crystals of vivianite (Plate I, Figs. 5, 6) and bone-shaped one is of random aggregates of the crystals. Under the microscope it is revealed that the nodular one includes a lot of clayey materials arranged concordantly with its radial structure, while tree-trunk-shaped one is free from inclusion. Figs. 5 and 6 are the microphotographs of thin section of vivianite, of nodular and tree-trunk-shaped ones respectively. The interior of each specimen is composed of fresh vivianite crystals, while its rim 2~3 mm. thick is composed of limonites and intermediate zone 2~

* The mammal fossils collected are revealed to be part of skeletons and five teeth of *Palaeoloxodon naumanni* and an antler of deer. They are being studied by Dr. F. Takai, Institute of Geology, University of Tokyo.

3 mm. thick of some yellow coloured hydrous ferric iron phosphate minerals.[6] Zones of limonite and yellow iron phosphate minerals are dark coloured in the micro-photographs.

Vivianite from Himeshima has following characters.

Colour: deep blue~yellowish. Transparent. Streak: blue. Hardness: 1.5~2. Luster: vitreous. Cleavage (010) easy. Specific gravity for the tree-trunk-shaped one: 2.66 at 17°C., by means of a picnometer. These properties agree well with those of usual vivianite.

Optical properties of the tree-trunk-shaped vivianite are as follows.

The indices of refraction measured by the dispersion method: α=1.587, β=1.607 and γ=1.631. 2V large. Pleochroism: X=blue, Y=colourless or yellowish and Z=yellowish. Optical orientations: X//b and Z$\wedge$c nearly 27°. These properties agree well with those of slightly oxidized vivianite.

Crystal morphology

Small but good idiomorphic crystals were found in the druses in some nodular specimens. Nearly ten crystals were measured on a V. Goldschmidt's two circle goniometer (Table 1). All of them are short prismatic, 1 mm. long and 0.3~0.5 mm. across. Seven crystal forms were observed, of which *b* (010) and *m* (110), gave good re-

Table 1. Two-circle angles of vivianite from Himeshima.

Forms	Measured value		Calculated value*		N**
	ρ	φ	ρ	φ	
b (010)	0°00′	90°00′	0°00′	90°00′	8
m (110)	54 18	〃	54 01	〃	9
w ($\bar{2}$01)	−90½°	34⅜°	−90 00	35 20	1
T (103)	90¼	29	90 00	30 12	1
x (221)	54	50⅛	54 01	50 03½	1

* Calculated on the basis of the values a : b : c = 0.7498 : 1 : 0.3509, β = 104°26′[2].

** Numbers of the faces measured.

flection, $w(\bar{2}01)$, $T(103)$ and $x(221)$, poor reflection and $d(801)$ and $V(441)$, very poor reflection. There are two types of crystal habit, the one consists of prisms and domes (Fig. 7) and the other of prisms and a hemi-pyramid (Fig. 8), with distinctly monoclinic symmetry.

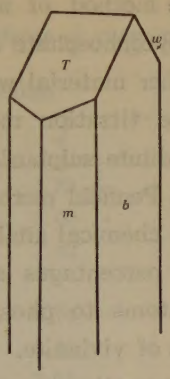

Fig. 7.

Fig. 8.

Figs. 7, 8. Crystals of vivianite from Himeshima.

Chemical analysis

Each of the two varieties of the vivianite from Himeshima, one is spherical nodule and the other is of tree-trunk-shape, was crushed to small cleavage flakes, which were hand-sorted under the binocular microscope to eliminate inclusions. The materials thus obtained were examined under the petrographic microscope with high-power objective, and it was found that the nodular one included fine grains of clay as not-ascertained impurities while the other contained no appreciable amount of impurity. Chemical analysis was carried out on each variety. An outline of the procedure will be described below.

After $H_2O(-)$ was determined, the material was dissolved by 6N nitric acid, insoluble part was filtered and determined. The filtrate was evaporated up and soluble silica was separated by using nitric acid and the filtrate was divided into two fractions. The one was used for the determinations of P_2O_5, Fe_2O_3 and Al_2O_3. After ferric nitrate solution had been added to the other fraction, Fe_2O_3, P_2O_5 and Al_2O_3 were separated by means of ammonium hydroxide. Then, MnO was determined by means of bromine water and ammonium hydroxide, CaO by ammonium oxalate and ammonium hydroxide, and MgO by oxine. After the filtrate had been evaporated up, Na_2O and K_2O were determined. P_2O_5 was separated

according to the method of ammonium molybdate and determined as magnesium pyrophosphate and then Fe_2O_3 and Al_2O_3 were determined. Another material was used for the determination of FeO according to the titration method with potassium permanganate solution with a dilute sulphuric acid, and another for total water according to the Penfield method.

The results of chemical analyses and the atomic ratios calculated from the weight percentages are listed in Table 2. The ratios of total metallic atoms to phosphoric are nearly equal to 3:2, the theoretical value of vivianite. But they have excess positive charge compared with negative charge of phosphoric, and the excess may be compensated by (OH) ion. Al_2O_3 of the nodular specimen may

Table 2. Chemical compositions and atomic ratios of the vivianites from Himeshima.

Nodular vivianite				Tree-trunk-shaped vivianite			
	Wt. %	Mol. prop.	Atom. rat.		Wt. %	Mol. prop.	Atom. rat.
P_2O_5	24.43%	.172		P_2O_5	26.48%	.189	
Al_2O_3	2.49	.024		Al_2O_3	0.59	.005	Al 0.01 }
Fe_2O_3	6.84	.043	Fe^{+3} 0.50 }	Fe_2O_3	14.00	.092	Fe^{+3} 0.89 } 2.90
FeO	30.04	.417	Fe^{+2} 2.24 } 3.01	FeO	29.30	.408	Fe^{+2} 1.99 }
MnO	0.24	.003	Mn, Mg 0.08 }	MnO	tr.	—	Mg 0.01 }
MgO	0.28	.007		MgO	0.10	.002	
CaO	0.06	.001	PO_4 2.00	CaO	0.12	.002	PO_4 2.00
Na_2O	tr.	—	OH 0.52	Na_2O	—	—	OH 0.70
K_2O	tr.	—		K_2O	—	—	
TiO_2	tr.	—		TiO_2	—	—	
SiO_2	non.	—		SiO_2	0.42	—	
SO_3	non.	—		SO_3	—	—	
Insol.	10.36	—		Insol.	0.06	—	
$H_2O(+)$	13.05	.725		$H_2O(+)$	16.11	.895	
$H_2O(-)$	12.65	.703		$H_2O(-)$	12.35	.686	
Total	100.44%			Total	99.89%		

Analysed by H. Minato. (1952 and 1955)

Table 3. X-ray powder patterns of vivianite.

Ashio mine		Himeshima		*hkl*
$I(FeK_\alpha)$	*d*	$I(FeK_\alpha)$	*d*	
1	8.85 Å	1/2	8.82 Å	
2	8.02	2	8.00	
3	7.49	3	7.42	
2	6.97			
10	6.79	10	6.74	(020)
		1/2	5.41	
1	4.93	2	4.91	(200)
1	4.58	1/2	4.55	(001)
1	4.38	1/2	4.37	
1	4.10	1	4.08	
1	3.866	1	3.861	($\bar{2}$01)
1	3.555	1/2	3.536	
1	3.311	1/2	3.285	(040)
2	3.217	1	3.214	
2	2.993	1	2.979	(201)
1	2.797	1/2	2.797	
1	2.737	1	2.722	
2	2.713	1	2.710	
1	2.644	1	2.645	
		1/2	2.598	
1	2.539	1	2.534	($\bar{2}$41)
		1/2	2.453	
1	2.430	1	2.432	(400), ($\bar{4}$01)
1	2.330	1	2.321	(002), ($\bar{1}$51)
1	2.233	1	2.233	
1	2.196	1/2	2.193	(060)
1	2.081	1/2	2.078	(260), (350)
1	1.924	1/2	1.927	($\bar{4}$02)
1	1.900			
1	1.887	1/2	1.885	(170)
1	1.682	1	1.681	(080)
1	1.673			($\bar{4}$42)
1	1.587	1/2	1.586	(531)

have been derived from mudstone inclusion. Considering the compensation by (OH) ion, the writer gives the following chemical formulas: for nodular specimen, $Fe^{+3}_{0.5}Fe^{+2}_{2.5}(PO_4)_{2.0}(OH)_{0.5}\cdot nH_2O$ and for tree-trunk-shaped specimen, $Fe^{+3}_{0.9}Fe^{+2}_{2.0}(PO_4)_{2.0}(OH)_{0.7}\cdot 7.9H_2O$. The H_2O content of the former could not be determined closely. These vivianites contain a considerable amount of ferric iron, owing to their oxidation.[2)]

X-ray powder patterns

As the tree-trunk-shaped vivianite was free from inclusions, it was chosen for examination of X-ray powder patterns by means of a Philips "Norelco" X-ray diffractometer. The observed intensities and measured spacings are listed in Table 3 together with those of the well crystallized specimen from the Ashio mine, Tochigi Prefecture. Their main features are in accordance with each other, but there are a few distinct differences in spacings. The ratio $Fe^{+2}:Fe^{+3}$ was equal to 11:5 for the specimen from Himeshima and 5:1 for that from Ashio.* The difference in the grade of oxidation of ferrous iron may be one of the cause of the difference between the two specimens in their X-ray powder patterns. As for the variance of crystal structure due to the oxidation, further study must be carried out, but the coincidence of the main features of the X-ray powder patterns suggests that the structure has not been affected so much by oxidation.

Acknowledgements

The writers wish to offer their sincere thanks to Professor Teiichi Ito of the Mineralogical Institute, University of Tokyo, for his kind help during the present work, especially in the X-ray investigation. Further acknowledgements are due to Mr. Yukio Takano of the Institute of Earth Science, College of General Education, University

* Analysed by H. Minato.

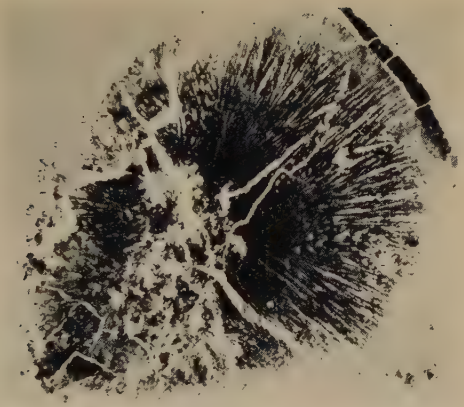

Fig. 5. Microphotograph of a thin section of nodular vivianite from Himeshima.
Dark coloured rim is of limonite and hydrous ferric iron phosphate.

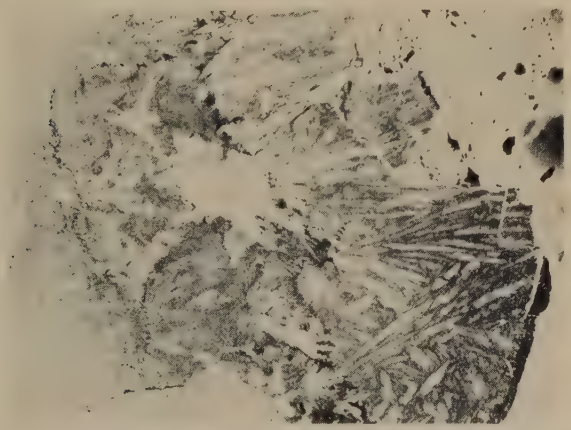

Fig. 6. Microphotograph of a thin section of tree-trunk-shaped vivianite cut perpendicular to the elongation.

of Tokyo for his assistance in X-ray experiments. They are indebted greatly to Professor Nobuo Katayama of College of General Education, University of Tokyo, for his useful suggestions on this manuscript. The writers are greateful to Mr. Kunihiko Muta of the Institute of Economic Geology, Faculty of Engineering, Kyushu University, Mr. Kanehisa Kônô of the Ooita Prefectural Office and Mr. Hanjirô Nishimura of the Himeshima Middle School to whom they owed the collection of the specimens used in this study.

REFERENCES

1) Benn, J. H.: Am. Miner., **20**, 311 (1935).
2) Dana's System of Mineralogy 7th. Ed., vol. II, 742 (1951).
3) Krotov, B. P.: Verh. Russ. Miner. Gesell., Ser. 2, **53**, 359 (1924).
4) Okamoto, Y.: Shuminochigaku, **2**, 127 (1953) (in Japanese).
5) Shannon, E. V.: Proc. U. S. Nat. Museum, **59**, 415 (1921).
6) Slavik, F.: Casopis Národniho Musea, **102**, 112 (1928).

Manuscript received January 17, 1956.

MINERALOGICAL JOURNAL, VOL. 1, NO. 6, pp. 348-358, JUNE, 1956

MAGNESIUM-RICH CHLORITE FROM THE WANIBUCHI MINE, SHIMANE PREFECTURE

TAKASHI SAKAMOTO

The Kawayama Mine, Nihonkōgyō Co.

and TOSHIO SUDO

Geological and Mineralogical Institute, Faculty of Science, Tokyo University of Education

ABSTRACT

Magnesium-rich chlorite occurs in the innermost fringe of the altered aureole around the gypsum deposits of the Wanibuchi mine, Shimane Prefecture, giving the following properties: the chemical composition, SiO_2 29.07, Al_2O_3 21.82, TiO_2 0.32, Fe_2O_3 0.83, FeO 3.67, MgO 29.90%, CaO 0.19, Na_2O tr., K_2O tr., $H_2O(+)$ 10.76, $H_2O(-)$ 2.76, Total 99.32%; the structural formula, $(Mg_{4.30}\ Fe''_{0.30}Fe'''_{0.06}\ Al_{1.28})\ (Al_{1.20}\ Si_{2.80})O_{10}(OH)_8$; the (004) spacing, 3.553 ± 0.002 Å. The thermal change with two steps was revealed in its dehydration curve, differential thermal analysis curve and the effect of heat on its X-ray powder diffraction; the last data also indicated that the chlorite powder lines disappear completely by the heat treatment at 860°C., and forsterite and enstatite phases occur during recrystallization at 1000°C..

Introduction

Galena, zincblende, chalcopyrite and pyrite ores are frequently found associated with one another forming hydrothermal replacement ore bodies in Tertiary tuffaceous or igneous rocks in Japan. Such ore deposits are commonly called as "Kuroko deposit", and gypsum deposits are often found associated with them. Clayey zones due to the alteration of wall rocks generally occur around those ore deposits. J. Takahashi and T. Yagi[5] (1930), for the first time, reported that a magnesium-rich clay is frequently found closely

associated with "Kuroko deposits". The present writers dealt with clays occurring around the gypsum deposit of the Wanibuchi mine, Shimane Prefecture. In this report will be given the mineralogical data of the altered zone with the results that a magnesium-rich clay mineral is found in this altered aureole, and that the principal alteration product can be identified as a magnesium-rich chlorite.

Reference specimens

Reference specimens are those collected from the altered area surrounding the gypsum deposit, from the innermost fringe progressing toward its outer zone, and they were numbered as (1), (2),...(7) following this sequence. The specimens collected from inner zones show commonly pale green colour, and are compact and massive, whereas those in outer zones show pale gray colour, and are porous and massive.

Preliminary tests

As far as these reference specimens concerned, both the degree of swelling in water and the colour-forming reaction with benzidine are negligible in the specimen from the innermost fringe, and they become remarkable progressing toward outer zones.

Each specimen with a definite weight was put into the agate mortar and mixed with a pH-indicator solution with a definite volume

Table 1. Staining test of clay specimens with the pH indicator solutions.

Specimens	(*P*)
No. 1	8.8~9.0
No. 2	9.0~9.2
No. 3	9.0~9.2
No. 4	8.6~8.8
No. 5	8.4~8.6
No. 6	8.6~8.8
No. 7	7.8~8.0

and ground for one minute. After this grinding, the indicator solution was soaked into a piece of absorbent cotton and the colour displayed on the cotton was compared with the colours illustrated on the chart of pH-values. The obtained pH values (P) are given in Table 1.

X-ray diffraction data

X-ray powder diffraction data was obtained by Philips Geiger counter X-ray diffractometer. The experimental conditions are as follows: filtered Cu radiation, 35 kV., 15 mA., scanning speed 2° per minute, time constant 4 seconds, receiving slit 0.006 inch, angular aperture 1°, goniometer radius 17 cm.. The X-ray powder diffraction data for the specimen collected from the innermost fringe agree with that of chlorite (Table 2, No. 1). The (004) spacing was

Table 2. X-ray diffraction data for two reference clay specimens.

No. 1			No. 7		
hkl	*d*	*I*	*hkl*	*d*	*I*
001	14.3 Å	5	001	15.2 Å	vs
002	7.14	10	003	5.06	vw
003	4.74	6	02, 11	4.46	s
020	4.58	3	005	3.22	vw
004	3.553	8.5	13, 20	2.57	w
005	2.846	2		2.38	vw
132, 20$\bar{2}$	2.583	2.5	22, 04	2.24	vw
13$\bar{2}$, 201	2.544	3		2.18	vw
132, 20$\bar{3}$	2.443	2.5	31, 15, 24	1.697	w
006	2.390	1		1.671	w
133, 20$\bar{4}$	2.258	1	06, 33	1.498	m
007	2.009	3			
135, 20$\bar{6}$	1.885	1			
137, 20$\bar{8}$	1.568	1			
060, 33$\bar{1}$, 331	1.536	2			
062, 331	1.504	1			
139, 208	1.396	1			

accurately determined from the record which was obtained under a slow scanning speed and unfiltered Cu radiation along with the standard quartz powder, and was revealed to be 3.553±0.001 Å, which agrees with those of magnesium-rich chlorites.

Though the X-ray diffraction data for specimens No. 2~No. 6 are rather similar to those of chlorite, they suggest that, in order from No. 2 toward No. 6, montmorillonite is included in gradual increasing abundance with the gradual reduction in the amount of chlorite, and the principal powder reflections of No. 7 agree with those of montmorillonite (Table 2, No. 7).

Weak powder reflections with long spacings

On close examination, weak X-ray powder reflections with long spacings were confirmed on most of the reference specimens. These spacings recorded under a slow scanning speed are listed in Table 3.

Table 3. The long spacings at about 30 Å and the 14 Å spacing.

Specimens	30 Å	14 Å
No. 1	——	14.5 Å
No. 2	——	14.5
No. 3	30~31 Å	14.8; 15.5
No. 4	30~31	14.4; 14.6
No. 5	30~31	14.4; 14.9; 15.6
No. 6	30~31	——
No. 7	30	——
No. 8	29~30	15.8; 16.4

The long spacings obtained are about 30 Å. It is very difficult to determine the type of these long spacings because of their diffuse and weak reflections, however, it can be expected that these long spacings are caused by a regular mixed-layer mineral between a chlorite with the cell hight of 14.3 Å and a montmorillonite with the cell hight of 15.4 Å. The line profile of the 14 Å reflection is simple in the cases of specimens No. 1 and No. 2, which are purely

composed of chlorite, whereas in the cases of specimens No. 3~ No. 6, the profile is complex accompanying small satellite peaks due to the second order reflection of the long spacing and/or the first order reflection of montmorillonite.

Chemical compositions

The five specimens of Nos. 1, 2, 3, 4, and 7 were analysed chemically and the results are tabulated in Table 4. The chemical composition of No. 1 is nearest to that of magnesium-rich chlorite, and can be plotted in the area of magnesium rich chlorites (penninite-leuchtenbergite-sheridanite-grochauite) of the Sudo's diagram[4]

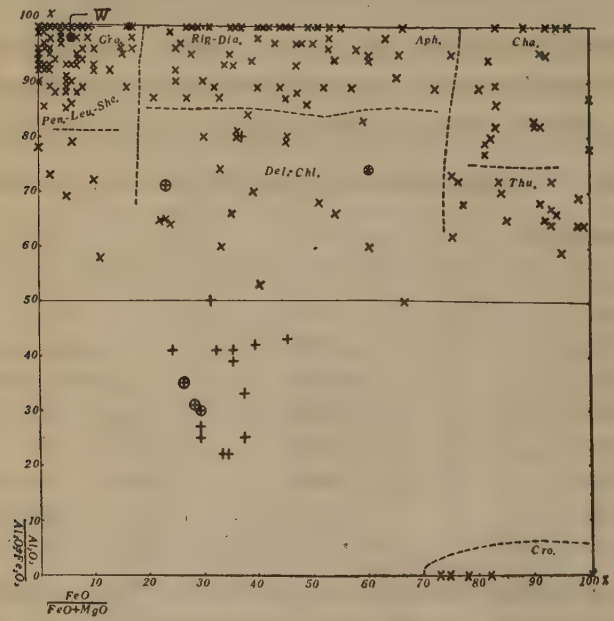

Fig. 1. Grouping of chlorites, celadonite and glauconite according to the ratios $Al_2O_3/(Al_2O_3+Fe_2O_3)$ and $FeO/(FeO+MgO)$.
×: chlorites. +: glauconite. ⊕: celadonite. Gro: grochauite. Pen: penninite. Leu: leuchtenbergite. She: sheridanite. Rip: ripidolite. Dia: diabantite. Aph: aphrosiderite. Del: delessite. Chl: chloropite. Cha: chamosite. Thu: thuringite. Cro: cronstedite. W: chlorite from Wanibuchi.

Table 4. Chemical compositions of clay specimens from the Wanibuchi mine.

	No. 1	No. 2	No. 3	No. 4	No. 7
SiO_2	29.07%	28.00%	28.67%	28.05%	53.69%
Al_2O_3	21.82	21.44	19.98	19.29	17.87
TiO_2	0.32	0.28	0.29	0.20	0.23
Fe_2O_3	0.83	2.44	1.82	1.50	1.65
FeO	3.67	3.11	2.26	1.52	0.66
MgO	29.90	30.75	31.15	31.02	2.63
CaO	0.19	0.40	0.40	0.37	2.04
Na_2O	tr.	—	0.13	0.10	0.20
K_2O	tr.	—	0.27	0.11	0.27
$H_2O(+)$	10.76	10.92	10.96	11.77	5.90
$H_2O(-)$	2.76	2.61	4.24	5.86	15.55
Total	99.32	99.95	100.17	99.79	100.69

(Fig. 1). The structural formula of No. 1 can be constructed from its chemical composition as follows:

$$(Mg_{4.30}Fe''_{0.30}Fe'''_{0.06}Al_{1.28})(Al_{1.20}Si_{2.80})O_{10}(OH)_8.$$

The slight differences between the chemical compositions of Nos. 1, 2, 3 and 4 may be caused by the gradual increasing abundance of montmorillonite which has been suggested by X-ray powder diffraction. The chemical composition of No. 7 agrees with that of montmorillonite giving the following structural formula;

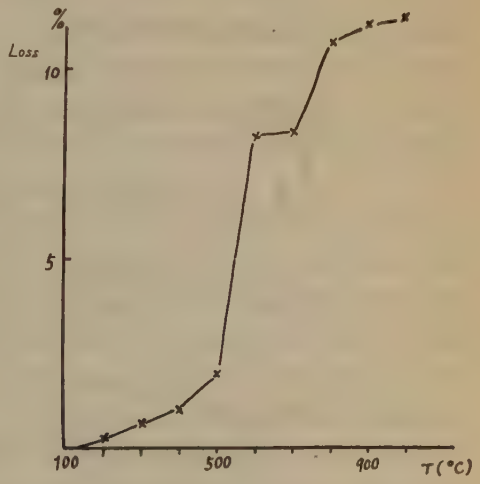

Fig. 2. Dehydration curve of specimen No. 1. This specimen was heated at every one hundred dgrees C. for one hour, then cooled and its loss of weight was determined.

$$(Al_{1.57}Fe'''_{0.09}Fe''_{0.04}Mg_{0.29})\ Si_{4.00}O_{10}(OH)_2\ (Na, K, Ca/2)_{0.33}.$$

Dehydration curve

The dehydration curve of specimen No. 1 is illustrated in Fig. 2. On the curve there are two steps due to loss of OH lattice water; one at about 600°C. and the other is at about 800°C..

Differential thermal analysis curves

The differential thermal analysis curves of the five specimens analysed chemically are as shown in Fig. 3. The d.t.a. curves of specimens Nos. 1, 2, 3 and 4 agree with one another and also with that of a magnesium-rich chlorite. The gradual increasing abundance of montmorillonite in order from No. 1 toward No. 4 gives rise to slight changes on these four curves, such as that the thermal peaks

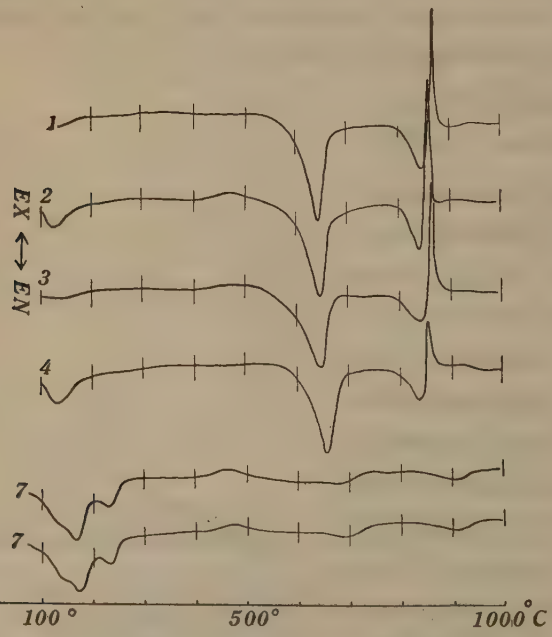

Fig. 3. Differential thermal analysis curves of clay specimens from Wanibuchi. Each numeral corresponds to that in Table 4.

become broader, and the first endothermic peak becomes more distinct, toward No. 4. The d. t. a. curve of No. 7 agrees with that of montmorillonite.

The structural changes taking place on heating

Specimen No. 1 was heated in the furnace under the heating rate of 10°C. per minute and cooled just immediately after the temperature attained to every one of the following temperatures as 300°C., 500°C., 700°C., etc., and analysed by X-ray (Table 5).

All the powder reflections of chlorite persisted in the specimen heated up to 600°C.. In the next step, the first order reflection increases remarkably in relative intensity in the specimens heated up to 800°C.. In the third step, the principal powder reflections of chlorite have perfectly disappeared in the specimen heated up to 840°C., and new additional powder reflections as 7.89 Å and 3.914 Å occur in this case. These additional powder reflections are inferred to be caused by an intermediate crystal configuration between chlorite and its firing product. The heat treatment at 860°C. caused the disappearance of the principal powder reflections of chlorite and the appearance of the principal powder reflections of the firing product as enstatite. In the final step, the heat treatment at 1000°C. gives rise to the powder reflections of forsterite.

The effect of the heat treatment was affected by the duration at maximum temperature. While the heating up to 600°C. did not give rise to any obvious change in the X-ray powder patterns, the duration for one hour at 600°C. caused the increase of the relative intensity of the first order reflection and the disappearance of the 7 Å and 4.7 Å reflections to give patterns corresponding to those at 700°C. in column (e), Table 5, which on the other hand still persisted when the specimen had been heated at 700°C. for one hour. Furthermore, when the specimen had been heated at 840°C. for one hour, the additional peaks as of 7.86 Å and 3.914 Å perfectly disappeared, and the similar patterns as those at 860°C. in column (h)

Table 5. The changes of X-ray powder patterns on heating of clay specimens from tne Wanibuchi mine.

(a)		(b) 300°C		(c) 500°C		(d) 600°C		(e) 700°C		(f) 800°C		(g) 840°C			(h) 860°C		(i) 1000°C		(j) 1000°C		(k) 1000°C	
d	*I*	*d*	*I*	*d*	*I*	*d*	*I*	*d*	*I*	*d*	*I*	*d*	*I*		*d*	*I*	*d*	*I*	*d*	*I*	*d*	*I*
14.3 Å	35	14.3 Å	40	14.3 Å	40	14.3 Å	55	14.15 Å	100	14.1 Å	100			F			5.12 Å	vw	5.12 Å	vw	5.12 Å	vw
												7.86 Å	10	E			4.33	vw	4.33	vw	4.33	vw
7.14	65	7.14	60	7.14	60	7.14	35			7.08	5			F			3.91	vw	3.91	w	3.91	w
4.74	40	4.75	40	4.75	40	4.74	30							F			3.73	vw	3.73	vw	3.73	vw
4.58	15	4.58	35	4.59	30	4.59	25	4.61	25	4.61	20	4.61	10	F			3.517	w	3.517	w	3.517	w
												3.914	5	E	3.300 Å	w						
3.553	55	3.555	55	3.556	55	3.548	30	3.531	15	3.531	5	3.531	5	E	3.151	m	3.151	m	3.151	ms	3.151	mw
2.846	15	2.846	15	2.846	15	2.838	20	2.829	20	2.829	20			F					3.005	w	3.005	vw
						2.653	10	2.673	15	2.669	10	2.680	15	E	2.873	vs	2.873	vs	2.869	vs	2.869	s
2.583	10	2.583	15	2.590	15	2.590	15	2.597	5	2.597	5			F			2.778	w	3.778	m	2.773	m
2.544	15	2.544	30	2.547	25	2.540	20	2.544	5	2.544	5	2.547	5						2.736	vw	2.736	vw
2.443	15	2.440	25	2.449	30	2.440	20	2.453	15	2.453	15	2.460	10	E	2.688	w	2.688	vw	2.696	vw	2.696	vw
2.390	5	2.381	10	2.390	10	2.398	5															
2.258	5	2.258	10	2.260	10	2.263	15	2.268	15	2.265	10	2.263	5	E	2.493	vs, b	2.493	vs, b	2.517	s	2.513	s
																			2.463	ms	2.466	s
2.009	20	2.004	25	2.013	25	2.002	20							F			2.258	w			2.252	mw, b
1.885	10	1.885	5	1.883	5	1.885	10												2.172	vw	2.174	vw
1.568	10	1.567	10	1.568	15									E			2.041	vw	2.026	w	2.023	w
1.536	15	1.536	20	1.538	20	1.537	25	1.545	15	1.545	15	1.546	5	E			1.967	vw	1.967	vw		
1.504	10	1.504	10	1.505	10	1.500	10												1.751	w	1.751	m
1.396	10	1.396	10	1.399	10	1.396	10														1.668	vw
																					1.482	w

(a) Unheated
(b)~(i) The specimen was heated up to the temperature mentioned in each column and cooled just after the temperature had been attained.
(j) Heated at 1000°C. for one hour. (k) Heated at 1000°C. for two hours.
The relative intensity was measured by the amplitude of peaks in the X-ray powder chart. The (001) reflection of the specimen heated at 700°C., was taken as standard and its intensity was assigned as 100. The same experimental condition was held throughout these experiments.
F: Principal powder reflections of forsterite. E: Principal powder reflections of enstatite.

Table 5 were obtained. The heat treatment at 1000°C. for one or two hours caused better development of the powder reflections of the firing products than those in column (i), Table 5.

Nomenclature

Many attempts have been made to classify the chlorite minerals. One of the important works is that of J. Orcel (1926) and recently structural studies have been taken into consideration by the workers as J. W. Gruner[2], G. W. Brindley and K. Robinson[1] and M. H. Hey[3]. In Japan, H. Shirozu is working on this problem (unpublished). It seems that many discussions will be continued till we shall get a proper classification.

As the purpose of this paper is to give the mineralogical property of the chlorite from the Wanibuchi mine, and not to attempt the thorough discussion of the chlorites, the writers will give this chlorite a name which is considered to be proper by referring to the recent literatures.

As to magnesium-rich chlorites, the following species names have been used for grouping; penninite, leuchtenbergite, sheridanite, grochauite. Among them, leuchtenbergite and sheridanite were studied by X-ray. In the scope of the recent data given by chemical as well as X-ray analyses, the magnesium-rich chlorite now under consideration is rather akin to leuchtenbergite or sheridanite than to the other two.

Acknowledgements

This study has been done on the Grant in Aid for Scientific Researches from the Ministry of Education in Japan.

REFERENCES

1) Brindley, G. W. and K. Robinson: "X-ray Identification and Crystal Structures of Clay Minerals", 197, (1951).
2) Gruner, J. W.: Amer. Miner., 29, 422, (1944).

3) Hey, M. H.: Miner. Mag., 30, 277, (1954).
4) Sudo, T.: Bull. Chem. Soc. Japan, 22, 25, (1949).
5) Takahashi, J. and T. Yagi: Journ. Jap. Assoc. Miner. Petrol. Econ. Geol., 4, 201; 5, 251, (1930).

Manuscript received February 29, 1956.

Mineralogical Journal Vol. 1, No. 6, pp. 359-371, June, 1956

EFFECTS OF CONSTITUENT CATIONS ON THE REFRACTIVE INDICES OF ORTHOPYROXENES

Fukutaro Hori

Institute of Earth Science, College of General Education, University of Tokyo

Abstract

Phenomenological equations for the refractive indices of orthopyroxenes are derived as a function of concentrations of constituent cations. Coefficients in these equations represent the coherent effects of individual cations on the refractive indices. The refractive indices calculated from the resulting equations are in rather good agreement with those observed. Thus probable changes in the refractive indices of the orthopyroxenes with ion substitutions are examined, in comparison with those of the clinopyroxenes.

Introduction

Relationships between the optical properties and the chemical composition of the clinopyroxenes were discussed elsewhere by adopting a statistical approach[10]. Orthopyroxenes have been worked out in terms of the same model. These works have a threefold purpose: to make it possible to place studies of changes in the optical properties of the ortho- and the clinopyroxenes with ion substitutions on a quantitative footing, to clarify differences in the degree of ionization of the same ions in these two pyroxenes, and to elucidate stability relationships of them from the energetic point of view.

In this contribution, an examination will be made only of the effects of individual cations on the refractive indices of the orthopyroxenes in comparison with those of the clinopyroxenes. The approach is consistently from the statistical point of view, no attempt being made to achieve physical rigor.

Approximate equations for the refractive indices of orthopyroxenes

Since a theoretical formula for the refractive index of such a silicate as pyroxenes is far too complicated to be derived in a rigorous fashion, this paper is concerned only with an approximation based on the assumption that the refractive index of a mineral depends entirely on the refractivities of individual ions and the relative orientations of these ions in the crystals. This does not necessarily require for the refractive index to be explicitly written in terms of variables characterizing the orientations. The formula should, however, be derived separately for every mineral having dissimilar atomic configurations.

No structural gap is proved to exist in the enstatite-ferrosilite series of orthopyroxenes[6),17)]. It is implicit then that the refractive index is written as a function of concentrations of every constituent ion in the crystals. And coefficients in the function represent the coherent contributions which the individual ions make to the refractive indices irrespectively of the properties and concentrations of coexisting ions in the crystals.

So far as a rough approximation is concerned, we have no evidence to doubt a linear correlation between the refractive indices and the chemical composition of the orthopyroxenes in the poly-dimensional space. Even if departures from linearity exist, terms of orders higher than the second in the functions are probably small enough so that they can be ignored. Let it be assumed then that the refractive indices are expressible as a linear combination of the individual effects of every ion. α, β and γ are thus given by

$$\alpha = C_\alpha + \sum_i a_{i\alpha} N_i, \qquad (1)$$

$$\beta = C_\beta + \sum_i a_{i\beta} N_i, \qquad (2)$$

$$\gamma = C_\gamma + \sum_i a_{i\gamma} N_i, \qquad (3)$$

where C refers to a constant, $a_{i\alpha}$, $a_{i\beta}$ and $a_{i\gamma}$ represent measures

for the effects of the ions of type i on the refractive indices α, β, γ, respectively, and N_i is the number of the ions per unit volume, and the sum over i is extended over all types of ion concerned.

Numbers of cations in the orthopyroxenes

The orthopyroxenes conform to the general structural formula $W_{1-p}(X, Y)_{1+p}Z_2O_6$[5]. Recently Hey[8] has discussed procedures for calculating the numbers of different ions in the unit cell from the cell volume and the density. In absence of these data for the orthopyroxenes, we cannot determine the values N_i which go into equations (1), (2) and (3). The data reported by Hess[6] are a few exceptions for this. With these materials, the present writer computed the numbers of oxygen ions in the unit cell to be 47.96, 47.75 and 48.75 for the samples Sh, W26 and 7666, respectively. Taking errors in the physical and the chemical measurements into account, we may safely say that there is no defect in oxygen positions in the orthopyroxenes. Then it is not unreasonable to assume, as we usually do, six oxygen ions as a basis for calculating ionic proportions in the crystal from the chemical analysis. Thus the numbers of ions are evaluated on the basis of six oxygen ions throughout this paper.

Procedures for putting each ion into Z, Y, X and W groups are practically the same as proposed by Kuno[18]. It is assumed from the outset that Z positions are to be filled up completely*. Enough Al is put into Z positions to make the number of ions there 2.000, the remainder being introduced into Y group. The majority of the orthopyroxenes examined contain sufficient amounts of Si and Al to satisfy the number required for Z group. However, this is not the case with some of them, with which Ti, Cr and Fe^{3+} are put into Z positions in this order until the number of ions there gets to 2.000, the remainder being introduced into Y group[9]. The constituents of

* In this paper physical reality of this assumption is not verified, even though it is of basic importance in the theory of the optical properties of crystals.

H_2O may be safely assumed not to enter the pyroxene structure. Thus the ions submitted into each group are as follows:

Z=Si, Al, Ti, Cr, Fe^{3+},
Y=Al, Ti, Cr, Fe^{3+},
X=Mg, Fe^{2+}, Mn, Ni,
W=Ca, Na, K.

Table 1. Ranges of ionic proportions in the orthopyroxenes used in regressions.

	Min.	Max.
Si	1.875	2.004
Al(4)*	0	0.125
Al(6)*	0	0.051
Ti	0	0.013
Cr	0	0.019
Fe^{3+}	0	0.061
Fe^{2+}	0.011	1.610
Ni	0	0
Mn	0	0.222
Mg	0.223	1.970
Ca	0.011	0.076
Na	0	0.025
K	0	0.003
W+X+Y	1.950	2.065

* Here and subsequently, the symbols Al(4) and Al(6) refer to Al in Z and Y positions respectively.

The proportions of the cations in the orthopyroxenes used in deriving the equations for the refractive indices vary between the extremities shown in Table 1.

Regressions for the refractive indices

Appreciable temperature modifications are unlike the situation with the orthopyroxenes[6) 17)]. Hence the regressions for the refractive indices were carried out together with plutonic, volcanic and metamorphic orthopyroxenes. When Al, Ti, Cr and Fe^{3+} are accommodat-

ed in both Z and Y positions, their effects in the respective positions should be considered separately. However, the entrance of Ti, Cr and Fe^{3+} into Z positions is still disputable. As an entry to the problem therefore the materials with which a sum of Si and Al in the Z group got to 2.000 were chosen to begin the regressions. The materials used in the regressions are shown in Table 2. The selection is arbitrary rather than exhaustive.

Table 2. Index to samples used in regressions.

Number	Rock	Classification	Source
1	Shallowater meteorite	Probably high temperature	Hess & Phillips[7], 1; Foshag[3]
2	Harzburgite	Plutonic	Kuno[13]
3	Websterite	Plutonic	Hess & Phillips[7], 4
4	Andesite	Volcanic	Kozu & Kawano[11], Kuno[17], 2
5	Andesite	Volcanic	Kuno[15]
6	Johnstown meteorite	Probably high temperature	Hess & Phillips[7], 10
7	Andesite	Volcanic	Kuno[15]
8	Dacite (pumice)	Volcanic	Kuno[12]
9	Dacite (pumice)	Volcanic	Taneda[22]
10	Dacite (tuff)	Volcanic	Kuno[13]
11	Andesite	Volcanic	Kuno[13]
12	Amphibolite	Metamorphic	Kuno[14]
13	Andesite	Volcanic	Kuno[16]
14	Contaminated Norite	Metamorphic	Henry[4], A
15	Hypersthene-grunerite-garnet rock	Metamorphic	Henry[4], B
16	Eulysite	Metamorphic	Henry[4], E
17	Eulysite	Metamorphic	Tsuru & Henry[23]

In view of the small amount of Cr present, it was included with Fe^{3+}*. From the same reason, the Na and K ions were added to each other to give a combined effect of these ions. The measure for the contribution which oxygen ions made to the refractive index

* This procedure leads to a negligibly different value of $a_{Fe^{3+}}$ from that which Fe^{3+} has otherwise.

was involved in the constant C.

Substituting the numbers of each type of cation into equations (1), (2) and (3) gives normal equations for α, β, and γ, respectively. Then the coefficients $a_{i\alpha}$, $a_{i\beta}$ and $a_{i\gamma}$ are determined by making use of the method of least squares. The calculations were carried through without regard to errors in chemical and optical measurements. Thus we have

$$\begin{aligned}\alpha=&1.6324-0.0802N_{Si}-0.0828N_{Al(4)}+0.0794N_{Al(6)}\\&+0.9731N_{Ti}+0.2230N_{Fe^{3+}}+0.1442N_{Fe^{2+}}+0.1518N_{Mn}\\&+0.0905N_{Mg}+0.1249N_{Ca}-0.1308N_{(Na+K)},\end{aligned}\qquad(4)$$

$$\begin{aligned}\beta=&1.8421-0.0830N_{Si}-0.00365N_{Al(4)}-0.0588N_{Al(6)}\\&+0.6354N_{Ti}+0.1374N_{Fe^{3+}}+0.0500N_{Fe^{2+}}+0.0510N_{Mn}\\&-0.0108N_{Mg}+0.0129N_{Ca}-0.1744N_{(Na+K)},\end{aligned}\qquad(5)$$

$$\begin{aligned}\gamma=&1.5786-0.0946N_{Si}-0.0232N_{Al(4)}+0.0647N_{Al(6)}\\&+0.6902N_{Ti}+0.1411N_{Fe^{3+}}+0.1121N_{Fe^{2+}}+0.1114N_{Mn}\\&+0.0501N_{Mg}+0.0835N_{Ca}-0.1056N_{(Na+K)}.\end{aligned}\qquad(6)$$

The birefringence is easily evaluated with the help of equations (4) and (6) to give

$$\begin{aligned}\gamma-\alpha=&-0.054+0.071N_{Si}+0.106N_{Al(4)}-0.015N_{Al(6)}\\&-0.283N_{Ti}-0.082N_{Fe^{3+}}-0.032N_{Fe^{2+}}-0.040N_{Mn}\\&-0.040N_{Mg}-0.041N_{Ca}+0.025N_{(Na+K)}.\end{aligned}\qquad(7)$$

Comparison of calculated refractive indices with observed values

The refractive indices calculated from the resulting equations are compared with the observed values for confirmation*. This has been done for the orthopyroxenes used in the regressions in Table 3. The values of the standard deviations indicate the closeness of fit of the equations to the original data; nothing suggests any serious

* In the following, figures for both the calculated and the observed refractive indices are rounded to the third decimal place.

Table 3. Calculated and observed refractive indices of the orthopyroxenes used in regressions.

	$\alpha_{calc.}$	$\alpha_{obs.}$	Δ_α	$\beta_{calc.}$	$\beta_{obs.}$	Δ_β	$\gamma_{calc.}$	$\gamma_{obs.}$	Δ_γ
1	1.653	1.651	+0.002	1.655	1.653	+0.002	1.660	1.659	+0.001
2	1.660	1.660	±0	1.663	1.664	−0.001	1.669	1.669	±0
3	1.670	1.668	+0.002	1.677	1.673	+0.004	1.679	1.679	±0
4	1.671	1.672	−0.001	1.676	1.677	−0.001	1.681	1.681	±0
5	1.675	1.676	−0.001	1.679	1.682	−0.003	1.685	1.687	−0.002
6	1.683	1.684	−0.001	1.692	1.692	±0	1.697	1.696	−0.001
7	1.686	1.686	±0	1.691	1.694	−0.003	1.697	1.698	−0.001
8	1.695	1.691	+0.004	1.703	1.701	+0.002	1.706	1.705	+0.001
9	1.693	1.692	+0.001	1.701	1.701	±0	1.706	1.706	±0
10	1.692	1.696	−0.004	1.700	1.705	−0.005	1.705	1.708	−0.003
11	1.695	1.696	−0.001	1.705	1.703	+0.002	1.707	1.708	−0.001
12	1.695	1.693	+0.002	1.701	1.704	−0.003	1.708	1.709	−0.001
13	1.705	1.702	+0.003	1.712	1.712	±0	1.717	1.715	+0.002
14	1.718	1.715	+0.003	1.731	1.728	−0.003	1.733	1.731	+0.002
15	1.735	1.738	−0.003	1.747	1.749	−0.002	1.754	1.755	−0.001
16	1.756	1.751	+0.005	1.761	1.760	+0.001	1.773	1.769	+0.004
17	1.753	1.755	−0.002	1.763	1.763	±0	1.770	1.773	−0.003
σ			±0.002			±0.002			±0.002

σ: standard deviation.

errors in the regression coefficients calculated.

The results should be checked against other orthopyroxenes. Since there were few data available for α and β refractive indices, the comparison has been made only for γ index of additional fifteen samples in Table 4.

It is easily seen from the tables 3 and 4 that deviations are rather random, and that there is nothing to suggest any notable departure from linearity in the index-composition relation*. Temperature modifications in the refractive index are unlike the situation with the orthopyroxenes within the limits of the present accuracy. α and β calculated are not unreliable in relation to γ observed.

* The existence of departures from linearity is of course not disproved in this fashion.

Table 4. Calculated and observed refractive indices of additional orthopyroxenes.

	$\alpha_{calc.}$	$\beta_{calc.}$	$\gamma_{calc.}$	$\gamma_{obs.}$	Δ_γ
18	1.663	1.667	1.670	1.670	±0
19	1.663	1.668	1.673	1.675	−0.002
20	1.665	1.673	1.676	1.680	−0.004
21	1.674	1.680	1.682	1.680	+0.002
22	1.677	1.683	1.686	1.683	+0.003
23	1.682	1.688	1.692	1.689	+0.003
24	1.683	1.691	1.693	1.692	+0.001
25	1.691	1.698	1.701	1.698	+0.003
26	1.689	1.696	1.701	1.699	+0.002
27	1.690	1.698	1.705	1.707	−0.002
28	1.704	1.713	1.719	1.721	−0.002
29	1.703	1.714	1.722	1.726	−0.004
30	1.709	1.718	1.728	1.730	−0.002
31	1.714	1.728	1.731	1.731	±0
32	1.714	1.724	1.732	1.735	−0.003
σ					±0.002

σ : standard deviation.

Note: Samples 18, 21, 23 and 25 contain 0.010, 0.002, 0.002 and 0.002 nickel, respectively. These were added to Fe^{2+}.

Thus equations (4), (5) and (6) turn out to be rather good approximations for α, β and γ, respectively, of the orthopyroxenes

Table 5. Calculated and observed refractive indices of orthopyroxenes with which addition of Al to Si does not get to 2.000.

	Ionic proportions alloted to Z group		$\alpha_{calc.}$	$\alpha_{obs.}$	Δ_α	$\beta_{calc.}$	$\beta_{obs.}$	Δ_β	$\gamma_{calc.}$	$\gamma_{obs.}$	Δ_γ
	Ti	Fe^{3+}									
33	0.002	0.037	1.685			1.685			1.687	1.677	+0.010
34	0.019	0	1.709			1.719			1.713	1.697	+0.016
35	0.011	0.010	1.718			1.723			1.722	1.703	+0.019
36	0.016	0	1.743			1.764			1.752	1.735	+0.017
37	0.005	0.034	1.719	1.720	+0.017	1.717	1.711	+0.006	1.723	1.719	+0.007
38	0.005	0.042	1.721	1.703	+0.018	1.720	1.713	+0.007	1.725	1.718	+0.007

without distinction of their thermal history.

Some orthopyroxenes do not carry sufficient amounts of Si and Al to make a sum of them 2.000. With these materials also the refractive indices were calculated by assuming that all of Ti, Cr and Fe^{3+} do not enter the Z positions, but the Y positions. The resulting values are shown in Table 5, together with the observed values. In striking contrast with the good agreement obtained above, the equations fail in these orthopyroxenes; sizes of deviations are rather large in relation to limits of errors of the present equations and measurements. This would imply that some proportions of Ti, Cr

Table 6. Index to samples in tables 4 and 5.

Number	Rock	Classification	Source
18	Pyroxenite	Plutonic	Hess[6], W26
19	Pyroxenite	Plutonic	Hess & Phillips[7], 2
20	Pyroxenite	Plutonic	Hess & Phillips[7], 5
21	Pyroxenite	Plutonic	Hess[6], 7666
22	Pyroxenite	Plutonic	Hess & Phillips[7], 7
23	Norite	Plutonic	Hess[6], EB38
24	Pyroxenite	Plutonic	Hess & Phillips[7], 8
25	Gabbro	Plutonic	Hess[6], EB130
26	Pyroxenite	Plutonic	Hess & Phillips[7], 12
27	Andesite	Volcanic	Ota[19], Kuno[17], 6
28	Dacite	Volcanic	Kuno[17], 14
29	Dacite (obsidian)	Volcanic	Kuno[17], 15
30	Micronoritic xenolith in norite	Plutonic	Walls[24], b
31	Norite	Plutonic	Walls[24], c
32	Eulysite	Metamorphic	Kuno[17], 19
33	Pyroxenite	Plutonic	Hess & Phillips[7], 3
34			Hess & Phillips[7], 11
35	Norite	Plutonic	Walls[24], a
36	Norite	Metamorphic	Walls[24], d
37	Noritic eucrite	Plutonic	Clavan, McNabb & Watson[2], 35-5
38	Norite	Plutonic	Clavan, McNabb & Watson[2], 35-6

and/or Fe^{3+} actually enter the Z positions, and that these ions as such have smaller refractivities than those in Y positions.

Changes in the refractive indices with ion substitutions

The present equations will permit prediction of changes in the refractive indices of the orthopyroxenes with ion substitutions. In Table 7 the probable changes have been set down. Table 7 gives also a comparison of the changes with the same type of ion substitution in the ortho- and clinopyroxenes[10]. The positive sign indicates an increase in the refractive indices with the ion substitution concerned, and the negative sign indicates a decrease.

Table 7. Changes in the refractive indices and in the birefringence of enstatite ($Mg_2Si_2O_6$: Op) and clinoenstatite ($Mg_2Si_2O_6$: Cp) with ion substitutions by 0.5 per cent.

		Substituting ions for Si or Mg							
		Al(4)	Al(6)	Ti	Fe^{3+}	Fe^{2+}	Mn	Ca	Na+K
Si	$\delta\alpha\times10^3$ (Op)	−0.026							
	$\delta\alpha\times10^3$ (Cp)	−0.40							
	$\delta\beta\times10^3$ (Op)	+0.79							
	$\delta\beta\times10^3$ (Cp)	−1.02							
	$\delta\gamma\times10^3$ (Op)	+0.33							
	$\delta\gamma\times10^3$ (Cp)	−0.23							
	$\delta(\gamma-\alpha)\times10^3$ (Op)	+0.35							
	$\delta(\gamma-\alpha)\times10^3$ (Cp)	+0.17							
Mg	$\delta\alpha\times10^3$ (Op)		−0.11	+8.83	+1.33	+0.54	+0.61	+0.34	−2.21
	$\delta\alpha\times10^3$ (Cp)		+1.10	+2.86	+1.75	+0.56	+0.35	+0.13	−1.67*
	$\delta\beta\times10^3$ (Op)		−0.48	+6.56	+1.48	+0.61	+0.62	+0.24	−1.61
	$\delta\beta\times10^3$ (Cp)		+1.98	+3.63	+2.25	+0.64	+0.29	+0.21	−3.46*
	$\delta\gamma\times10^3$ (Op)		+0.15	+6.40	+0.91	+0.62	+0.61	+0.33	−1.56
	$\delta\gamma\times10^3$ (Cp)		+1.01	+2.35	+1.26	+0.64	+0.40	+0.22	−1.06*
	$\delta(\gamma-\alpha)\times10^3$ (Op)		+0.25	−2.43	−0.42	+0.08	±0	−0.01	+0.65
	$\delta(\gamma-\alpha)\times10^3$ (Cp)		−0.09	−0.51	−0.49	+0.08	+0.05	+0.09	+0.62*

* Tentatively assigned as a mean of the values for Na and K.

α is decreased by a substitution of Si by Al, while β and γ are increased. The net result of this substitution is to raise the birefringence. α, β and γ are raised by a substitution of Mg by Ti and Fe^{3+}, the effect of Ti being most remarkable of all the constituents. The birefringence is decreased by their entrance into Mg positions. Al(6) causes γ to increase, while it causes α and β to decrease. The resultant effect of Al(6) on the birefringence is to raise it. Fe^{2+} and Mn have rather similar refractivities to each other. Na and K have a combined effect that causes the refractive indices to decrease and the birefringence to increase.

Discussion

In the statistical method of approach taken here, we can have some informations about relative values of the refractivities of individual ions in the pyroxenes, although we cannot estimate absolute values of them. Comparing the present results with those for the clinopyroxenes reveals some degree of difference in the rate of changes in the refractive indices of the two pyroxenes with the same type of ion substitution. This would imply that the refractivity of a given ion may depend on environments in which it is placed.

This appears to be at variance with the Lorenz-Lorentz formula* obtained in connection with the electromagnetic theory. Essentially this formula is significant only if the atomic polarizabilities of the same particles in different compounds remain unaltered so that atom-refraction can be assigned unique values. The additivity law of the refraction is in fact found fairly fulfilled in many chemical compounds as well as mixtures**.

---

* See, for example, H. A. Lorentz: Theory of electrons, Teubnov, esp. pp. 137-150 (1909).

** For example, compare the values of the atomic polarizabilities of the alkali and halide ions determined by Schockley[21] so that the mean square deviation of dielectric constants from the observed values is a minimum with the values for the free ions as estimated by Pauling[20].

On the other hand, it is also found that the additivity law is only of approximate character even for such a simple ionic crystal as alkali halides*.

From the quantum mechanical point of view, this contradiction to the additivity law is rather reasonable, for a bonding of atoms arises from electrons shared between two or more atoms and thus the states of the valency electrons in the compounds should differ from those in the free atoms**.

Thus it is safe to say that the refractivity of a given ion is variable depending on whether it is a constituent of the orthopyroxenes, or of the clinopyroxenes. If this is really the case with the pyroxenes, the degree of ionization of the ions in the two pyroxenes may be different from each other, owing to an admixture of homopolar bonding.

As with the equations for the refractive indices of the clinopyroxenes, the present equations hold on the assumptions which have not been verified in a satisfactory fashion. Nevertheless, their quantitative features remain fairly applicable to discussing changes in the refractive indices of the orthopyroxenes with ion substitutions. This suggests that we may speak with some significance of the refractivity of individual ions in the pyroxenes.

Acknowledgements

The writer is grateful to Professors Nobuo Katayama, and Shuichi Iwao, Institute of Earth Science, College of General Education, the University of Tokyo, for comments on the manuscript. He wishes to acknowledge his appreciation to Professor Hisashi Kuno, Dr. Akiho Miyashiro, and Mr. Masao Yamasaki, Geological Institute,

* According to Born and Heisenberg[1], different refractivities for a given ion are obtained depending on the particular salt used.

** In the optical range of frequency and in the solid silicates only the electronic polarizability is active, whereas the ionic and the orientational polarizabilities give no contribution to the refractive index.

Faculty of Science, the University of Tokyo, for stimulating discussions of the problem. Special thanks are due to Miss Yoshiko Miyata of our Institute, who helped in the numerical calculation. The financial support for this research was obtained from the Japanese Government Expenditure for Scientific Research for which he is duly grateful.

References

1) Born, M. and W. Heisenberg: Zeit. f. Physik, **23**, 388, (1924).
2) Clavan, W., W. M. McNabb and E. H. Watson: Amer. Mineral., **39**, 566 (1954).
3) Foshag, W.: Amer. Mineral., **25**, 779 (1940).
4) Henry, N. F. M.: Mineral. Mag., **24**, 221 (1935).
5) Hess, H. H.: Amer. Mineral., **34**, 621 (1949).
6) Hess, H. H.: Amer. Jour. Sci., Bowen Volume, 173 (1952).
7) Hess, H. H. and A. H. Phillips: Amer. Mineral., **25**, 271 (1940).
8) Hey, M. H.: Mineral. Mag., **30**, 481 (1954).
9) Hori, F.: Mineral. Jour., **1**, 109 (1954).
10) Hori, F.: Sci. Papers Coll. Gen. Educ. Univ. Tokyo, **4**, 71 (1954).
11) Kozu, S. and Y. Kawano: Jap. Ass. Mineral. Petro. Econ. Geol., Jour., **6**, 273 (1931).
12) Kuno, H.: Imp. Acad. Tokyo, Proc., **14**, 218 (1938).
13) Kuno, H.: Imp. Acad. Tokyo, Proc., **17**, 204 (1941).
14) Kuno, H.: Jap. Acad., Proc., **23**, 114 (1947).
15) Kuno, H.: Jap. Acad., Proc., **23**, 117 (1947).
16) Kuno, H.: Geol. Soc. Amer., Bull., **61**, 957 (1950).
17) Kuno, H.: Amer. Mineral., **39**, 30 (1954).
18) Kuno, H.: Amer. Mineral., **40**, 70 (1955).
19) Ota, R.: Geol. Surv. Japan, Rept. No. 151, 33 (1952).
20) Pauling, L.: Proc. Roy. Soc. (London), **114A**, 181, (1927).
21) Shockley, W.: Phys. Rev., **70**, 105 (A) (1946).
22) Taneda, S.: Geol. Soc. Japan, Jour., **52**, 61 (1946).
23) Tsuru, K. and N. F. M. Henry: Mineral. Mag., **24**, 527 (1937).
24) Walls, R.: Mineral. Mag., **24**, 165 (1935).

Manuscript received March 15, 1956.

Mineralogical Journal, Vol. 1, No. 6, pp. 372-394, June, 1956

OPTICAL PROPERTIES AND UNIT CELL DIMENSIONS OF CORDIERITE AND INDIALITE

Toshimichi Iiyama

Tokyo Medical and Dental University

Abstract

The optical properties and unit cell dimensions of cordierite were studied for the purpose of presenting methods for the estimation of the $(Fe^{+2}+Mn)$: $(Mg+Fe^{+2}+Mn)$ ratio and the degree of distortion (deviation from the hexagonal indialite structure) of the minerals. The results are summarized in determination diagrams given in this paper. The unit cell dimensions of indialite were compared with those of cordierites and the relation was established that the unit cell volume of cordierite increases with the increase in the degree of distortion. The study also revealed that the optical properties of volcanic cordierite differ considerably from those of high cordierites inverted from low subdistortional cordierites by heating and the cause of this difference is discussed.

Introduction

It was previously reported by A. Miyashiro, the present writer and others[12,13] that crystals of cordierite composition, $(Mg, Fe^{+2})_2Al_4Si_5O_{18}$, have at least three modifications: indialite, high cordierite and low cordierite.

Recently, Miyashiro[14] found that there are all gradations from hexagonal indialite to orthorhombic cordierite through the distortion of the hexagonal lattice, probably caused by the order-disorder distribution of Si and Al atoms. He also studied the thermal relations existing among these polymorphs (Table 1).

However, the method of estimating the chemical compositions of these polymorphic forms and the degree of distortion of the indialite structure has not been worked out. The writer studied the optical

Table 1. Polymorphic relation of cordierite and indialite.

Relation obtained in 1955[13]		System	Relation revised in 1956[14]		Distortion index
Form	Characterizing properties		Form	Characterizing properties	
High indialite	Hexagonal symmetry, lower refractive indices than those of low indialite.	Hexagonal	High indialite	Hexagonal symmetry	0°
High cordierite	Pseudohexagonal symmetry, lower refractive indices than those of low cordierite, refr. indices showing no change on heating at 1000°C. for 10 min.	Pseudo-hexagonal	High subdistortional cordierite	Intermediate distortion index. Refr. indices showing no change on heating at 1000°C. for 10 min.	0.01°~0.27°
			High perdistortional cordierite	Large distortion index. Refr. indices showing no change on heat ng at 1000°C. for 10 min.	0.29°~0.31°
Low cordierite	Pseudohexagonal symmetry, considerable decrease in refr. indices on heating. Higher ref. indices than those of high cordierite.	Pseudo-hexagonal	Low subdistortional cordierite	Intermediate distortion index. Considerable decrease in refr. indices on heating.	0.01°~0.28°
			Low perdistortional cordierite (?)	Large distortion index. Decrease in refr. indices on heating.	0.29°~0.31°
Low indialite	Hexagonal symmetry, higher refr. indices than those of high indialite.	Hexagonal	?		0°

properties and unit cell dimensions of cordierite and indialite with the intention to throw light on this point.

This study revealed the manner of change in unit cell dimensions accompanying the transformation of these minerals and the relation between the shape of the unit cell and the distortion index Δ. This index was defined by Miyashiro[14] as the angular distance between the diffraction angle for the (131) line and the mean for (421) and (511) for Cu K_{α_1} radiation, namely,

$$\Delta = 2\theta_{131} - (2\theta_{421} + 2\theta_{511})/2 \text{ (for Cu } K_{\alpha_1} \text{ radiation).}$$

Samples studied

Cordierite samples were selected from the collection of the Geological Institute, University of Tokyo. Some of them were purified by heavy solutions and analysed chemically by T. Katsura and H. Haramura of Tokyo Institute of Technology.

Table 2 gives the compositions of analysed samples and Table 3

Table 2. Chemical compositions of cordierite.

No.	2	3	6	7	8	12
SiO_2	47.09%	48.52%	46.75%	48.04%	47.43%	46.99%
Al_2O_3	34.86	35.25	33.64	33.41	33.34	32.72
TiO_2	0.03	tr.	none	0.06	0.03	0.10
Fe_2O_3	0.11	0.41	0.72	0.01	0.07	0.16
FeO	2.59	3.43	4.89	5.04	4.91	7.12
MnO	0.05	0.08	0.31	0.20	0.12	0.42
MgO	11.92	10.40	10.43	10.32	9.70	8.38
CaO	0.04	tr.	0.04	0.04	0.04	0.06
Na_2O	0.78	0.13	0.24	1.12	0.61	0.85
K_2O	tr.	0.16	0.56	0.30	tr.	0.30
P_2O_5	—	0.01	0.02	—	—	—
$H_2O(+)$	2.21	2.06	2.63	1.81	2.74	3.07
$H_2O(-)$	0.65	0.12	0.10	0.23	1.01	0.05
Total	100.33%	100.57%	100.33%	100.58%	100.00%	100.22%

Analyst: Nos. 2 and 8 by H. Haramura and T. Katsura, and Nos. 3, 6, 7 and 12 by H. Haramura.

Table 2 (continued). Number of atoms per unit cell.
(Calculated from chemical analysis, the number of oxygen atoms per cell being taken to be 18.)

No.	2	3	6	7	8	12	18
Si	4.79	4.91	4.81	4.90	4.92	4.89	
Al (4*)	1.21	1.09	1.19	1.10	1.08	1.11	
Al (6*)	2.97	3.07	2.93	2.92	3.00	2.97	
Ti	0.00	—	—	0.01	0.00	0.01	
Fe^{+3}	0.01	0.03	0.05	0.00	0.01	0.01	
Fe^{+2}	0.22	0.29	0.42	0.43	0.43	0.62	
Mn	0.00	0.01	0.00	0.02	0.01	0.04	
Mg	1.81	1.57	1.60	1.57	1.50	1.30	
Ca	0.00	—	0.00	0.01	0.00	0.01	
Na	0.15	0.01	0.05	0.24	0.12	0.17	
K	—	0.01	0.07	0.03	—	0.04	
$H_2O(+)$	0.75	0.70	0.90	0.62	0.95	1.06	
$H_2O(-)$	0.22	0.04	0.03	0.08	0.35	0.02	
$\frac{Fe^{+2}+Mn}{Mg+Fe^{+2}+Mn}\times 100$	11.1	15.9	21.9	22.2	22.6	33.6	70.3

The chemical composition of specimen No. 18 (cordierite from Sugama) was taken from the data obtained by M. Sambonsugi.[19]

* Coordination number.

gives the localities and the modes of occurrence of both the analysed and the unanalysed samples.

Samples of pure Mg-indialite were obtained through synthetic procedure and those containing some Fe, from natural cordierites through heat treatment. The specimen for Fe-indialite was not available and only its X-ray diffractogram supplied by J. F. Shairer and H. S. Yoder of the Geophysical Laboratory, Washington, was used.

Optical properties of cordierite

It was previously stated that the optical properties of cordierites belonging to one of the modifications change continuously with their

Table 3. Localities and modes of occurrence of the sample studied.

No.	Locality	Mode of occurrence	Reference	Note
1	Risör, Norway	Pegmatite ?	Structure analysis: Byström[1]	
2	Laramie Range, Wyoming, U. S. A.	Metamorphic cordierite deposit	Newhouse and Hanger[15]	New analysis, Laramie No. 2
3	Orijärvi, Finland	Metamorphic rock	Eskola[4]	New analysis
4	Guilford, Conn., U. S. A.	Pegmatitized gneiss	Farrington,[5] Oppenheimer[16]	
5	Seto, Arii-mura, Mie Pref., Janan	Granite porphyry		
6	Hitachi Mine, Ibaragi Pref., Japan	Cordierite-quartz vein	Takeuchi[24]	New analysis
7	Mont Bity, Madagascar	Quartz vein	Duparc, Wunder and Sabot[3]	New analysis
8	New Haven, Conn., U. S. A.	Pegmatite		New analysis
9	Unity, Maine, U. S. A.	Pegmatite		
10	Micanite, Col., U. S. A.	Pegmatite		
11	Laramie Range, Wyoming, U. S. A.	Metamorphic cordierite deposit	Newhouse and Hanger[15]	New partial analysis, Laramie No. 1
12	Haddam, Conn., U. S. A.	Pegmatite	Oppenheimer[16]	New analysis
13	Takato, Nagano Pref., Japan	Pegmatite		
14	Sori, near Ashio Mine, Tochigi Pref., Japan	Biotite-cordierite hornfels	Kikuchi[11]	
15	Nyoidake, Kyoto, Japan	Biotite-cordierite hornfels		
16	Volcano Asama, Nagano Pref., Japan	Xenolith in andesite	Hussak[6], Yamasaki[25]	
17	Micanite, Col., U. S. A.	Pegmatite	Heinrich[7]	
18	Sugama, Fukushima Pref., Japan	Pegmatite	Sambonsugi[19]	New analysis
19	Yagenyama, near Naegi, Gifu Pref., Japan	Protolithionite-topaz bearing metasomatic vein in granite	Shibata[21]	

chemical compositions but differ discontinuously from those of other modifications. In fact, there is a tendency that the refractive indices of high (volcanic) cordierites are a little lower than those of low (metamorphic and pegmatitic) cordierites. However, there is a wide variation in refractive indices among the latter varieties and the constants of the materials having the same composition often take different values from specimen to specimen. This situation is probably due to the existence of per- and subdistortional types among the low modification and makes it difficult to obtain a simple relation between the optical constants and the composition of the modifications, unless we pay special attention to the structural relationship existing between these types.

The perdistortional type of cordierite was defined by Miyashiro[14] as the variety having maximum degree of deviation from the hexagonal indialite structure and the subdistortional type as having the intermediate structure between the perdistortional and the indialite structure. In general, the former variety has lower refractive indices than the latter. Miyashiro's study also indicated that low subdistortional cordierites are transformed into high perdistortional ones upon heating.

Therefore, there is a possibility of avoiding the difficulty mentioned above, if we deal always with the optical properties of heat-treated samples.

Optical properties after heating

The optical properties of analysed cordierites after heating at 1000°C. for 10 minutes are tabulated in Table 4, and in Fig. 1 are plotted against the atomic ratios, $\frac{Fe^{+2}+Mn}{Mg+Fe^{+2}+Mn} \times 100$. As seen from the figure, the refractive indices after heating vary regularly with the ratios. Miyashiro found that low subdistortional cordierites do not always change completely to high perdistortional cordierites under the above experimental conditions. But the present study indicates that the difference in the refractive indices, especial-

Table 4. Optical properties of analysed cordierites.

No.	$\frac{Fe^{+2}+Mn}{Mg+Fe^{+2}+Mn}\times 100$	Δ before heating	Before heating				After heating				Locality
			α	β	γ	$2V_X$	α	β	γ	$2V_X$	
2	11.1	0.27°	1.534	1.539	1.543	77°	1.525	1.530	1.535	77°	Laramie (No. 2)
3	15.9	0.27	1.534	1.536	1.545	89	1.528	1.534	1.539		Orijärvi
6	21.9	0.25	1.542	1.546	1.551	68	1.531	1.537	1.541		Hitachi
7	22.2	0.26	1.539	1.544	1.547	68	1.530	1.536	1.541		Mont Bity
8	22.6	0.27	1.538	1.542	1.554	72	1.532	1.537	1.543		New Haven
12	33.6	0.12	1.551	1.560	1.562	42	1.536	1.543	1.548	66	Haddam
18	70.3	0.12	1.560	1.574	1.578	55	1.550	1.555	1.558	67	Sugama
11	31*	0.27	1.542	1.548	1.555	77°~88°	1.536	1.543	1.550		Laramie (No. 1)

* Estimated by partial analysis of FeO.

ly β, of heated samples and those of high perdistortional cordierites is too small to detect optically the incompletion of the inversion, if there is any. Therefore, the refractive indices after heating at 1000°C. for 10 minutes can practically be used for the estimation of the composition. The compositions of the unanalysed samples given in the second column of Table 5 were thus estimated from Fig. 1.

Optical properties before heating

Optical properties before heating are tabulated in Tables 4 and 5, β-index of each of the samples arbitrary classified into four groups according to their distortion indices, is plotted against the atomic ratio $\frac{Fe^{+2}+Mn}{Mg+Fe^{+2}Mn}\times 100$ as shown in Fig. 2. In the same figure plotted the data of heated and volcanic cordierites for comparison.

Table 5. Optical properties of unanalysed cordierites.

No.	$\frac{Fe^{+2}+Mn}{Mg+Fe^{+2}+Mn}\times 100$	Δ before heating	Before heating				After heating			Locality
			α	β	γ	2Vz	α	β	γ	
1	6	0.25	1.530	1.535	1.539		1.522	1.527	1.532	Risör
4	21	0.24	1.539	1.546	1.550		1.533	1.536	1.538	Guilford
5	21	0.27	—	1.542	—		—	1.536	—	Seto
9	30	0.26	1.546	1.550	1.556		1.536	1.541	1.544	Unity
10	31	0.27	1.542	1.546	1.552		1.536	1.541	1.547	Micanite (country rock)
13	34	0.22	1.552	1.557	1.560		1.538	1.543	1.549	Takato
14	37	0.27	1.547	1.551	1.554		1.540	1.544	1.548	Sori
15	39	0.24	1.549	1.556	1.561	96°~114°	1.541	1.545	1.548	Nyoidake
16	40?	0.30	1.537	1.542	1.545		1.537	1.542	1.545	Volc. Asama
17	50	0.13	1.560	1.568	1.572		1.544	1.549	1.556	Micanite (pegmatite)
19	80?	0.23	1.558	1.570	1.576		—	—	—	Yagenyama
a	28.7		1.530	1.534	1.537	99°				
b	43.9		—	1.544	—	94°				

a: By Ichimura[8] on a specimen from biotite-hornblende andesite at Kasyô-to.
b: By Ossan[17] on a specimen from garnet-cordierite-mica andesite at Cabo de Gata.
Errors in refractive indices measurements are approximately within ±0.003.

As seen from the figure, the refractive indices of cordierites of nearly the same Δ-value show regular variation with the composition, and the difference in Δ-values of about 0.01° causes a change in refractive indices of about 0.002 for large-Δ cordierites and about

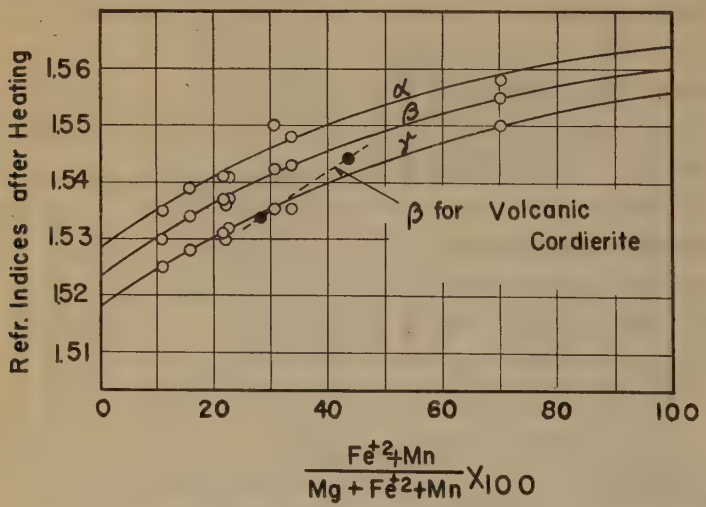

Fig. 1. Refractive indices of analysed cordierites after heating.

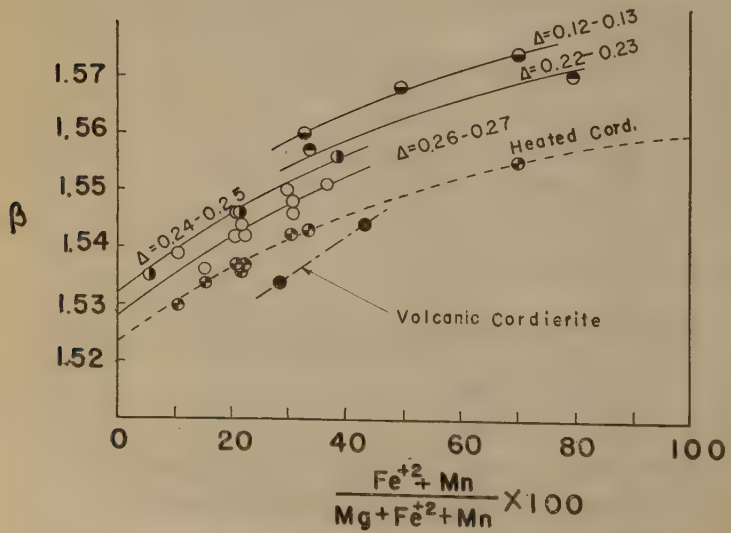

Fig. 2. Refractive index β of cordierites before heating.

0.0005 for small-Δ cordierites.

The refractive indices of volcanic cordierites (compiled from the literatures and given in Table 5) are considerably lower than those of metamorphic and pegmatitic cordierites which have been heated and inverted to high perdistortional cordierites. The difference will be discussed in a later paragraph.

Decrease in refractive indices of cordierite on heating

The amount of decrease in refractive indices on heating at 1000° C. for 10 minutes, as obtained from Tables 4 and 5, are given in Table 6. Fig. 3 shows the relation between the amount of decrease in refractive indices and the distortion index Δ before heating and also between Δ and $2V_X$.

Table 6. Distortion index, Δ, before heating and the amount of decrease in refractive indices on heating at 1000°C. for 10 minutes.

No.	Δ	Decrease in refr. indices α	β	γ	Locality
1	0.25°	0.008	0.008	0.007	Risör
2	0.27	0.009	0.009	0.008	Laramie (No. 2)
3	0.27	0.006	0.002	0.006	Orijärvi
4	0.24	0.006	0.010	0.012	Guilford
5	0.27	—	0.006	—	Seto
6	0.25	0.011	0.009	0.010	Hitachi
7	0.25	0.009	0.008	0.006	Mont Bity
8	0.27	0.006	0.005	0.011	New Haven
9	0.26	0.010	0.009	0.012	Unity
10	0.27	0.006	0.005	0.005	Micanite*
11	0.27	0.006	0.005	0.005	Laramie (No. 1)
12	0.12	0.015	0.017	0.014	Haddam
13	0.23	0.014	0.014	0.011	Takato
16	0.29	0.000	0.000	0.000	Volcano Asama**
17	0.13	0.016	0.019	0.016	Micanite***
18	0.12	0.010	0.019	0.020	Sugama

* Country rock. ** High perdistortional cordierite. *** Pegmatite.

Unit cell dimensions of cordierite

Indexing of X-ray powder diffraction patterns

The X-ray powder diffraction patterns of cordierites were obtained by a Norelco X-ray diffractometer operated under the following conditions: speed of goniometer scanning, ¼°/min. in 2θ; scale factor, 4 or 8; multiplier factor, 1; time constant, 4 sec.; chart driving speed, ½ inches/min.; radiation, filtered Cu K_α (λ=1.54050 Å for K_{α_1}).

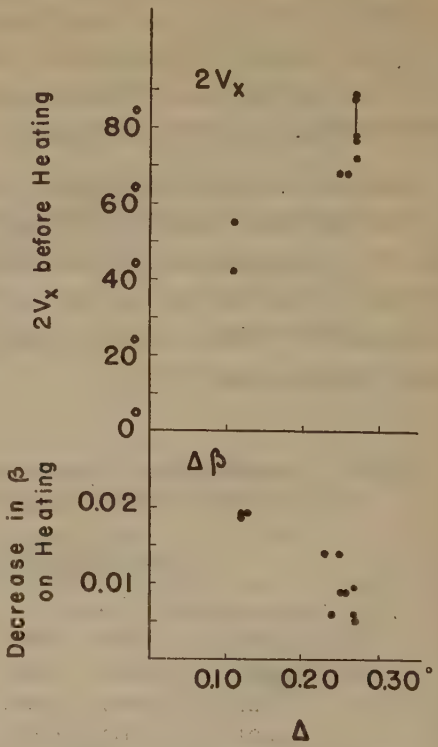

Fig. 3. Relation between $2V_x$ before heating, decrease in refractive index β on heating and index of deformation of cordierites.

G. Donnay and J. D. H. Donnay[3] proposed to read the diffraction angle 2θ at the mid-point of the peak width at approximately two-thirds of the peak height. However, as some of the peaks in the pattern under consideration are so close together (overlap partly one another), the measurement at the mid point of the peak width tends to be inaccurate. The reading was therefore made at the top of each peak. The diffraction angles 2θ, thus measured, were calibrated by those of silicon or rock salt used as internal standards. Silicon gives sharp and well resolved peaks, but unfortunately the diffraction from its (111) planes falls on the characteristic peaks of cordierite, (222) and (420) (2θ=28.2°–28.5° for CuK_α). The rock salt

Table 7. X-ray powder diffraction data of cordierite from Risör.

hkl	$2\theta_{obs}$	Q_{obs}	Q_{calc}	$2\theta_{calc}$	*I*
$044_{\alpha 2}$	54.50			54.49	7
044	54.37	35181	35181	54.37	11
$624_{\alpha 2}$	54.21			54.21	9
624	54.09	34847	34849	54.09	19
$1000_{\alpha 2}$	53.72			53.73	3
1000	53.60	34265	34280	53.61	6
$334_{\alpha 2}$	50.82			50.82	4
334	50.69	30886	30874	50.68	8
$351_{\alpha 2}$	50.60			50.59	3
351	50.45	30613	30629	50.46	6
$243_{\alpha 2}$	48.71			48.71	3
243	48.60	28543	28553	48.61	5
533	48.42	28346	28360	48.43	10
713	48.24	28142	28139	48.23	8
442	47.13	26940	26953	47.14	3
$730_{\alpha 2}$	46.67			46.65	2
730	46.51	26275	26302	46.53	6
820	46.40	26158	26163	46.40	5
224	44.21	23868	23879	44.22	3
$242_{\alpha 2}$	43.28			43.31	4
242	43.17	22811	22839	43.20	9
$532_{\alpha 2}$	43.11			43.11	4
532	43.01	22653	22646	43.00	7
$314_{\alpha 2}$	42.90			42.90	3
314	42.80	22439	22425	42.79	8
622	41.47	21128	21136	41.48	7
133	40.44	20135	20133	40.44	3
423	40.30	20001	19994	40.29	3
513	40.23	19935	19911	40.21	3
$004_{\alpha 2}$	38.55			38.55	12
004	38.46	18284	18284	38.46	24
332	37.20	17148	17161	37.21	2
$040_{\alpha 2}$	37.00			37.00	3
040	36.91	16891	16897	36.92	6
$620_{\alpha 2}$	36.60			36.63	3

hkl	$2\theta_{obs}$	Q_{obs}	Q_{calc}	$2\theta_{calc}$	*I*
620	36.52	16548	16565	36.54	6
132	34.01	14415	14419	34.01	3
$422\alpha_2$	33.95			33.92	5
422	33.84	14254	14279	33.84	12
512	33.77	14216	14197	33.74	27
$131\alpha_2$	29.65			29.66	30-15
131	29.59	10991	10991	29.59	70-40
$421\alpha_2$	29.45			29.47	30-20
421	29.39	10846	10852	29.40	65-40
511	29.29	10774	10769	29.28	60-45
222	28.43	10164	10166	28.43	85
402	28.28	10059	10056	28.28	70-50
022	26.40	8789	8795	26.41	50
$312\alpha_2$	26.35			26.34	40-70
312	26.29	8717	8712	26.28	70-90
112	21.69	5959	5970	21.71	85-120
002	18.98	4575	4571	18.97	20
020	18.21	4214	4224	18.23	12
310	18.04	4136	4141	18.05	27
110	10.46	1398	1399	10.46	100
200	10.36	1371	1371	10.36	100

$$Q=\frac{1}{d^2}\times 10^5$$

Calculation is based on the wave length of Cu $K\alpha_1$ in the angular range of 25°~50° in 2θ, on Cu K_α in the range of 10°~25° in 2θ, and on the unit cell dimensions (1) in Table 9.

was therefore, more suitable for the present study.

The standard indexing was made on the sample from Risör, Norway, which was also used by A. Byström[1] on his structure analysis of the mineral. The indexing was checked by comparing the measured intensity of diffractions on the diffractogram with that given by Byström[1] on single crystal of cordierite. The result is shown in Table 7. The agreement between the observed and calculated values of 2θ and $Q(=1/d^2)$ is satisfactory for such a complicated diffraction pattern as shown in Fig. 4. The indexing was also attempted

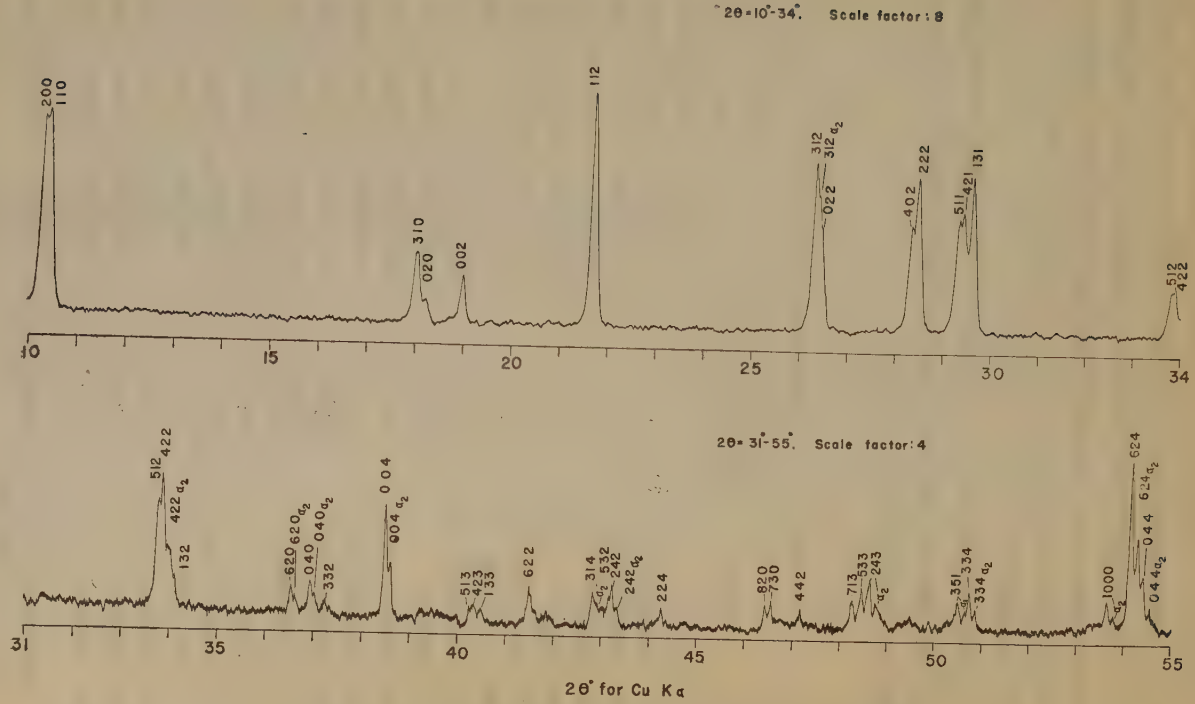

Fig. 4. X-ray powder diffractogram of cordierite from Risör

for cordierites of different compositions so as to confirm the space group of these samples, but this was not successful because of the complicated nature of the diffraction patterns. It can only be stated here that there is no distinct diffraction which is at variance with the space group, Cccm, given by A. Byström[1] and by K. Takane and T. Takeuchi.[2,3]

The diffraction patterns of cordierites vary one another depending on the degrees of distortion and compositions. Some of the diffraction data are given in Table 8.

Table 9. Unit cell dimensions of cordierites

	No.	Locality	$\frac{Fe^{+2}+Mn}{Mg+Fe^{+2}+Mn}\times 100$	Δobs	Δcalc	Unit cell dimensions a_0	b_0	c_0
Unit cell dimensions of unheated cordierites	1	Risör	6	0.25	0.25	17.07_9Å	9.73_1Å	9.35_4Å
	2	Laramie (No. 2)	11.1	0.27	0.27	17.09_5	9.72_8	9.34_5
	3	Orijärvi	15.9	0.27	0.26_5	17.09_9	9.73_3	9.33_6
	4	Guilford	21	0.25	0.24_5	17.10_0	9.74_7	9.32_7
	6	Hitachi	21.9	0.24	0.24	17.10_9	9.74_8	9.32_9
	7	Mont Bity	22.2	0.26	0.26	17.11_0	9.74_0	9.32_9
	8	New Haven	22.6	0.27	0.27	17.11_5	9.73_8	9.33_3
	11	Laramie (No. 1)	31	0.27	0.27	17.14_7	9.76_1	9.31_8
	12	Haddam	33.6	0.12	0.12	17.02_3	9.76_2	9.32_9
	13	Takato	34	0.23_5	0.23_5	17.09_5	9.76_1	9.33_1
	16	Volc. Asama	40 (?)	0.29	0.29	17.18_6	9.76_9	9.31_5
	18	Sugama	70.3	0.12	0.12	17.14_7	9.83_0	9.30_1
	19	Yagenyama	80(?)	0.23	0.23	17.28_8	9.85_4	9.29_2
Unit cell dimensions of heated cordierites	1	Risör	6	0.28	0.28_5	17.10_2	9.72_8	9.35_4
	2	Laramie (No. 2)	11.1	0.27_5	0.27_5	17.09_6	9.74_0	9.34_1
	7	Mont Bity	22.2	0.29	0.28_5	17.11_1	9.73_9	9.33_1
	12	Haddam	33.6	0.16	0.15_5	17.04_7	9.76_2	9.32_4
	13	Takato	34	0.27	0.26_5	17.15_2	9.76_1	9.32_7
	18	Sugama	70.3	0.21	0.20_5	17.18_2	9.80_4	9.30_6

Accuracy of unit cell dimension is approximately ±0.007Å for a_0 and b_0, and ±0.005Å for c_0.

Table 8. X-ray powder dif

No.	2			6			12		
Locality	Laramie No. 2			Hitachi			Haddam		
$\frac{Fe^{+2}+Mn}{Mg+Fe^{+2}+Mn}\times 100$	11.1			21.9			33.6		
Δ_{obs}	0.27			0.24			0.12		
hkl	$2\theta_{obs}$	$2\theta_{calc}$	*I*	$2\theta_{obs}$	$2\theta_{calc}$	*I*	$2\theta_{obs}$	$2\theta_{calc}$	*I*
$044_{\alpha 2}$	54.55	54.55	6	54.54	54.53	9	54.54	54.54	19
044	54.39	54.39	12	54.38	54.38	18	54.38	54.38	38
$624_{\alpha 2}$	54.23	54.24	9	54.27	54.26	35	—	—	—
624	54.09	54.09	18	54.12	54.11	60	54.25	54.25	39
225	—	—	—	—	—	—	—	—	—
1000	53.57	53.56	6	53.53	53.52	13	—	—	—
$334_{\alpha 2}$	—	—	—	—	—	—	—	—	—
334	—	—	—	50.70	50.71	15	50.76	50.75	18
732	—	—	—	—	—	—	—	—	—
$351_{\alpha 2}$	50.60	50.60	12	—	—	—	—	—	—
351	50.47	50.48	18	50.39	50.38	10	—	—	—
604	—	—	—	—	—	—	—	—	—
641	50.22	50.24	3	—	—	—	50.26	50.24	6
350	—	—	—	—	—	—	49.32	49.32	12
640	49.22	49.21	3	—	—	—	49.18	49.21	16
910	—	—	—	—	—	—	49.02	49.04	18
$243_{\alpha 2}$	48.72	48.75	6	48.71	48.71	8	—	—	—
243	48.61	48.63	12	48.59	48.59	13	48.59	48.58	37
533	48.43	48.44	9	48.42	48.42	10	48.51	48.50	34
134	—	—	—	—	—	—	—	—	—
713	48.22	48.22	4	48.22	48.22	6	48.37	48.40	19
424	—	—	—	—	—	—	—	—	—
821	—	—	—	—	—	—	47.60	47.61	6
$442_{\alpha 2}$	47.24	47.27	3	—	—	—	—	—	—
442	47.14	47.15	6	47.11	47.09	5	—	—	—
802	—	—	—	—	—	—	46.91	46.91	18
150	—	—	—	—	—	—	—	—	—
730	46.51	46.51	6	46.45	46.45	7	46.58	46.60	15
224	—	—	—	44.27	44.27	5	44.31	44.32	3
820	—	—	—	—	—	—	—	—	—
333	—	—	—	—	—	—	43.24	43.26	15
404	—	—	—	—	—	—	—	—	—

242	43.18	43.21	9	43.17	43.15	15	43.16	43.13	25	
532	43.00	43.00	9	42.95	42.96	14	43.03	43.04	25	42
314	42.79	42.80	9	—	—	—	—	—	—	42
800	—	—	—	—	—	—	—	—	—	
042	41.82	41.84	3	41.77	41.77	4	41.75	41.74	6	
712	—	—	—	—	—	—	—	—	—	42
622	41.44	41.47	6	41.45	41.44	11	41.57	41.58	12	41
133	—	—	—	—	—	—	—	—	—	
423	40.29	40.31	3	40.31	40.30	7	40.37	40.38	15	
513	40.18	40.21	3	40.22	40.22	7	—	—	—	
204	39.93	39.95	3	—	—	—	—	—	—	
$004_{\alpha 2}$	38.55	38.57	12	38.66	38.55	15	38.69	38.69	10	
004	38.48	38.48	27	38.54	38.54	32	38.59	38.59	21	38
332	—	—	—	37.17	37.19	3	—	—	—	
040	36.90	36.93	6	36.86	36.85	7	—	—	—	36
620	36.52	36.52	3	36.48	36.48	11	36.63	36.62	30	36
313	—	—	—	—	—	—	—	—	—	
$422_{\alpha 2}$	33.95	33.93	6	—	—	—	—	—	—	
422	33.85	33.85	9	33.82	33.83	43	33.88	33.90	52	33
132	—	—	—	—	—	—	—	—	—	33
512	33.73	33.74	18	33.73	33.73	45	—	—	—	
$131_{\alpha 2}$	—	—	—	—	—	—	—	—	—	29
131	29.60	29.60	45	29.54	29.55	80	29.52	29.52	45	29
421	29.38	29.39	51	29.34	29.36	92	29.44	29.43	50	29
511	29.28	29.27	66	29.26	29.25	100	29.37	29.37	60	
$222_{\alpha 2}$	—	—	—	—	—	—	—	—	—	
222	28.43	28.45	75	28.42	28.43	98	28.47	28.45	60	28
402	28.26	28.27	47	28.27	28.28	50	28.40	28.38	40	
022	26.40	26.43	78	26.42	26.41	43	26.40	{26.41	80	26
312	26.29	26.29	72	26.31	26.29	57		26.35}		
112	21.71	21.73	115	21.74	21.74	64	21.77	21.76	60	21
002	18.97	18.99	46	19.00	19.01	18	19.04	19.04	12	19
020	18.23	18.24	9	18.19	18.20	10	—	—	—	
310	18.04	18.04	23	18.03	18.02	32	18.08	18.09	25	18
110	10.46	10.46	100	10.43	10.44	80	10.46	10.44	90	10
200	10.35	10.35	66	10.35	10.34	100	10.39	10.40	100	
Δ_{calc}	0.27			0.24$_5$			0.12			

Unit cell dimensions of cordierites

The unit cell dimensions were calculated from the diffraction data with the result given in Table 9. In Fig. 5 these dimensions are plotted against the atomic ratio, $\frac{Fe^{+2}+Mn}{Mg+Fe^{+2}+Mn}\times 100$, and the curves representing the relation between the cell dimensions and the composition are shown.

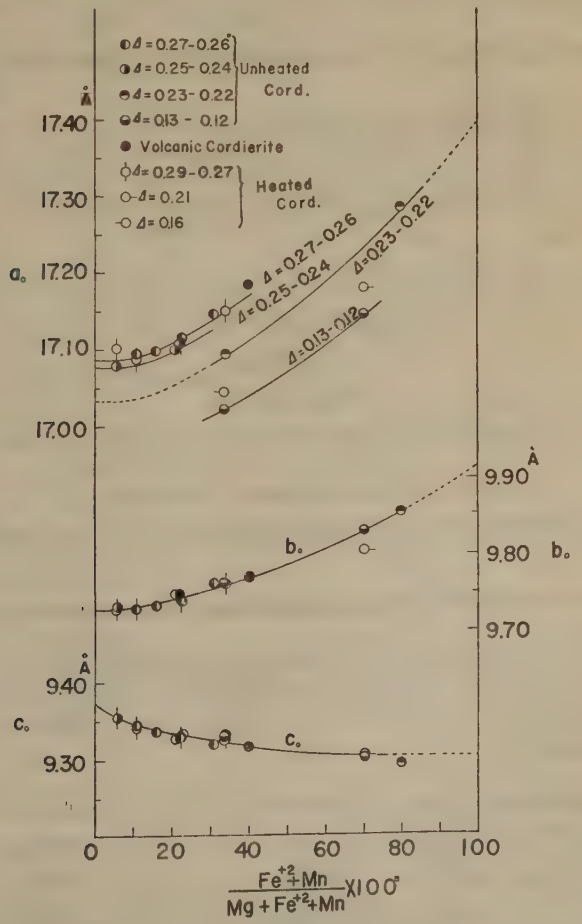

Fig. 5. Unit cell dimensions of cordierites.

The cell dimensions b_0 and c_0 are dependent only on the composition but apparently independent of the distortion index; a single smooth curve can be drawn for the variation of each of them. On the contrary, a_0 varies both with the composition and the distortion index. Therefore, four separate cuves are drawn in the figure, each corresponding a different value of the distortion index. This result shows that the diffraction angle 2θ for (004) (2θ=38.4°–38.7° for Cu K_{α_1}) is suitable for estimating the $\frac{Fe^{+2}+Mn}{Mg+Fe^{+2}+Mn}\times 100$ value. The relation between $2\theta_{004}$ and the composition is shown in Fig. 6.

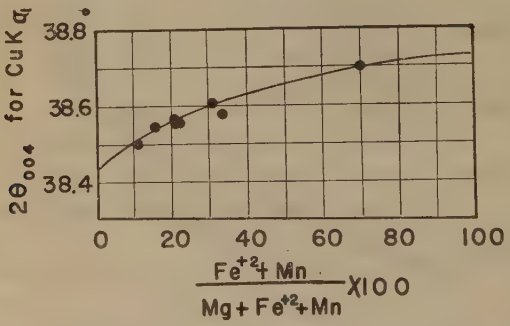

Fig. 6. $2\theta_{004}$ for Cu K_{α_1} of chemically analysed cordierites.

Unit cell dimensions of indialites

Unit cell dimensions of Mg-indialites formed at various temperatures

Magnesium indialites were synthetized at various temperatures

Table 10. Unit cell dimensions of Mg-indialites formed at various temperatures.

Temperature of formation	a_0	c_0
1350±20°C	9.77_7 Å	9.35_8 Å
1250±20	9.77_7	9.35_8
1200±20	9.77_7	9.35_8
1100±20	9.74_2	9.39_4
1000±20	9.74_2	9.39_4

(1000°, 1100°, 1200°, 1250° and 1350° C.) by devitrification of glass having the composition of Mg-indialite. The X-ray diffraction angles for CuK_{α_1} radiation were measured and the cell dimensions are given in Table 10. The table shows that the cell dimensions of Mg-indialites formed above 1200° C. are different from those formed below this temperature. The cell dimensions listed in the table also differ from those of β-indialite obtained previously (a_0=9.76$_2$Å c_0=9.34$_9$ Å).[12][13]

Unit cell dimensions of Fe-indialite and indialites of intermediate compositions

Unit cell dimensions of Fe-indialite and of indialites of intermediate compositions are calcululated from the X-ray diffractograms as given in Table 11. These data indicate that the cell dimensions

Table 11. Unit cell dimensions of Fe-indialite and indialites of intermediate composition.

$\frac{Fe^{+2}+Mn}{Mg+Fe^{+2}+Mn}\times 100$	a_0	c_0
100 (synthetic)	9.86$_0$ Å	9.28$_5$ Å
70.3[1]	9.80$_1$	9.31$_0$
33.6[2]	9.74$_2$	9.34$_5$

1) Obtained from natural cordierite, No. 18 by heating at 1200°C. for 10 minutes.
2) Obtained from natural cordierite, No. 12 by heating at 1360°C. for 10 minutes.

Several unindexed peaks appeared in the X-ray diffraction patterns of these samples, probably due to the partial disintegration of natural cordierite on strong heating.

of indialites inverted from cordierites differ from those estimated by interpolation based on the data for the synthetic Mg-indialite and Fe-indialite. This difference may be due to partial disintegration of Fe bearing crystals on strong heating at 1360° C. and at 1200°C. for 10 minutes and also to imperfect inversion from cordierite to

indialite. It is also possible that the crystals inverted from natural cordierite may belong to another polymorphic form of indialite.

Discussion

Accuracy of estimated composition and distortion index by optical and X-ray methods

Assuming that the errors attached to the measurements of refractive indices and 2θ are $\pm$ 0.003 and $\pm 0.02°$ respectively, we can give the estimated values of composition and of Δ with the following uncertainties.

Estimated value of Δ by X-ray diffratcfometer..... $\pm$ 0.02°.

Estimated value of composition, $\frac{Fe^{+2}+Mn}{Mg+Fe^{+2}+Mn}\times 100$,

by $2\theta_{004}$ ..... $\pm$ 10%,

by refractive indices after heating (1000° C. for 10 min.) ..... $\pm$ 5~8%,

and by refractive indices before heating ..... accuracy depending greatly on that of estimated Δ-values.

Change in unit cell dimensions accompanying the change in the distortion index

From the data given in Table 9 we can determine the amounts of change of the unit cell dimensions accompanying the transition from the mineral with a lower distortion index to the one with a higher index. As the result of the calculation an increase of about 0.1° in the distortion index corresponds to an increase of about 0.4% of cell dimension a_0 while b_0 and c_0 apparently remain unchanged.

These data also bring out the fact that the minerals with lower distortion indices have smaller unit cell volumes. It follows then that high pressure favours the formation of indialite and cordierites with lower distortion indices, though the effect may be small.

In view of the symmetry relation between indialite and cordierite

as well as of the conditions of their occurrence, it is supposed that indialite may differ from cordierite in the distribution of Si and Al among tetrahedral positions, the distribution may be disordered in indialite and ordered in cordierite. Any mineral with disordered distribution of atoms will generally have a larger unit cell volume than the mineral of the same composition with an ordered structure. However, indialite has a smaller unit cell volume than cordierite. A more interesting fact is that the specific gravity of Mg-indialite may be smaller than that of glass of the same composition, as is indicated by a higher refractive index of the glass ($n = 1.550$ by Karkhanavala and Hummel[10], and $n=1.556$ by Iiyama[9]) than those of the crystal ($n_{max} = 1.528$, $n_{min} = 1.524$ by Rankin and Merwin[18]). It may, therefore, be concluded contrary to the general case, the atomic packing is increasing with the increase of disordering of atoms in this case.

K. Sugiura and T. Kuroda[22] reported the results of the thermal expansion measurements with the X-ray diffractometer on synthetic indialite. They stated that the mineral shows the thermal shrinkage on heating in the temperature range of 20°~500°C.. This peculiar behavior of thermal expansion of indialite seems to be in harmony with the above conclusion.

Relation between the distortion index and deviation from the hexagonal symmetry

The degree of deviation of cordierite from the hexagonal symmetry can be expressed in terms of the distortion index Δ. If the hexagonal lattice is described in reference to the orthorhombic setting of axes, it is obvious from a simple geometrical relation that $\sqrt{3}\, b_0$ should be equal to a_0. The deviation from the hexagonal symmetry adequately expressed with the value of $a_0 - \sqrt{3}\, b_0$ which should become 0 for indialite. These values were calculated from the unit cell data of cordierites and are plotted against the Δ-values as shown in Fig. 7. The linear variation of Δ-values with the deviation from the hexagonal symmetry is evident.

Thus, for example, in order to transform the cordierite with $\Delta=0.12°$ to indialite, it is necessary to shorten the a_0 length by about 0.7%, and the perdistortional cordierite ($\Delta=0.30°$) deviates from the hexagonal indialite by about 1.6% of the a_0 length.

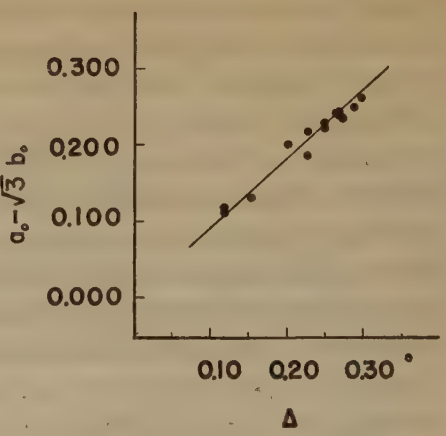

Fig. 7. Relation between the index of distortion and the deviation from the hexagonal symmetry of cordierites.

On volcanic cordierite

The optical properties of volcanic cordierite indicate that it differs from the high perdistortional cordierite inverted from a low subdistortional one.

This difference may be ascribed to imperfect inversion of low subdistortional cordierite upon heating. However, in view of the errors in the optical measurements and also of the fact that the physical properties of high perdistortional cordierite inverted from a low subdistortional one do not change appreciably upon further heating until it has been transformed into high indialite, it is possible that the volcanic cordierite may belong to another polymorphic form.

Acknowledgements

A part of this study was carried out in the Geological Institute, University of Tokyo, and the rest in the Research Institute of Dental Materials of Tokyo Medical and Dental University.

The writer wishes to express his gratitude to Prof. Teiroku Sueno of the latter University for putting various facilities of his laboratory at the writer's disposal.

The writer's thanks are due to Prof. Emeritus Seitaro Tsuboi, Prof. Hisashi Kuno, Dr. Akiho Miyashiro, Mr. Masao Yamasaki and Mr. Shigeo Aramaki of the Geological Institute, University of Tokyo, for their criticism and encouragement. He is also greatly obliged to Prof. Isi Miura of Tokyo Medical and Dental University for the use of the vacuum furnace of his laboratory, to Prof. Miyoji Sambonsugi of Fukushima University for the permission of using his unpublished data on Fe-rich cordierite from Sugama and to Prof. Takashi Katsura and Mr. Hiroshi Haramura of Tokyo Institute of Technology for undertaking the chemical analysis of the samples.

Part of the expenses for this study was defrayed from the Grant in Aid for Scientific Researches from the Ministry of Education.

References

1) Byström, A: Arkiv. Kemi, Miner. Geol., **15** B, No. 12 (1942).
2) Donnay, G. and J. D. H. Donnay: Am. Jour. Sci., Bowen Volume, 115 (1952).
3) Duparc, L., M. Wunder and R. Sabot: Neues Jahrb., Referate II, 364 (1911).
4) Eskola, P.: Comm. Géol. Finlande Bull., **40** (1914).
5) Farrington, O. C.: Am. Jour. Sci., 3d Ser., **43**, 13 (1892).
6) Hussak: Seitzungsber. d. K.K. Akad. D. Wiss. in Wien, Math.-Naturwiss. Klasse, **88**, 332 (1883).
7) Heinrich, E. Wm.: Am. Miner., **35**, 173 (1950).
8) Ichimura, T.: Kazan **3**, 1 (1936). (in Japanese)
9) Iiyama, T.: Jap. Acad. Proc., **31**, 166 (1955).
10) Karkhanavala, M. D. and F. A. Hummel: Am. Ceram. Soc. Jour., **36**, 389 (1953).
11) Kikuchi, Y.: Jour. Imp. Univ. Tokyo, **3**, 325 (1890).
12) Miyashiro, A. and T. Iiyama: Jap. Acad. Proc., **30**, 746 (1954).
13) Miyashiro, A., T. Iiyama, M. Yamasaki and T. Miyashiro: Am. Jour. Sci., **253**, 185 (1955).
14) Miyashiro, A: Cordierite-indialite relations. Am. Jour. Sci. (in press) (1956).
15) Newhouse, W. H. and A. F. Hangar: Wyoming Geol. Surv. Bull., 41 (1949).
16) Oppenheimer, L.: Neues Jahrb. Referate I,175 (1914).
17) Ossan A.: Deutsche Geol. Gesel. Zeitschr., **40**, 694 (1888).
18) Rankin, G. A. and H. E. Merwin: Am. Jour. Sci., 4th ser., **45**, 301 (1918).
19) Sambonsugi, M.: Iron-rich cordierite structurally close to indialite (in press) (1956).

20) Schairer, J. F. and K. Yagi: Am. Jour. Sci., Bowen Volume, 471 (1952).
21) Shibata, H.: Jour. Geol. Soc. Japan, 46, 69 (1939) (in Japanese).
22) Sugiura, K. and T. Kuroda: Jour. Ceram. Assoc. Japan, 63, 579 (1955) (in Japanese).
23) Takane, K. and T. Takeuchi: Jour. Japnese Assoc. Miner. Petr. Econ. Geol., 14, 101 (1936) (in Japanese).
24) Takeuchi, T.: Jour. Japanese Assoc. Miner. Petr. Econ. Geol., 14, 109 (1935) (in Japanese).
25) Yamasaki, N.: Jour. Geol. Soc. Japan, 2, 397 (1890) (in Japanese).

Manuscript received May 19, 1956.

Mineralogical Journal, Vol. 1, No. 6, pp. 395-397, June, 1956

SHORT COMMUNICATIONS

CHLORITE FROM THE HITACHI MINE, IBARAGI PREFECTURE

Hiroshi Sato and Toshio Sudo

Geological and Mineralogical Institute, Faculty of Science, Tokyo University of Education

Introduction The reference specimen was kindly supplyed by T. Takeyasu of the Hitachi Mine, Ibaragai Prefecture, to the writers. Their attention had been drawn by the microscopic study over the fact that the specimen is purely composed of chlorite showing dark green coloured hexagonal flakes (Fig. 1). The present paper describes its mineralogical data.

Mode of occurrence The specimen occurs as dark green coloured

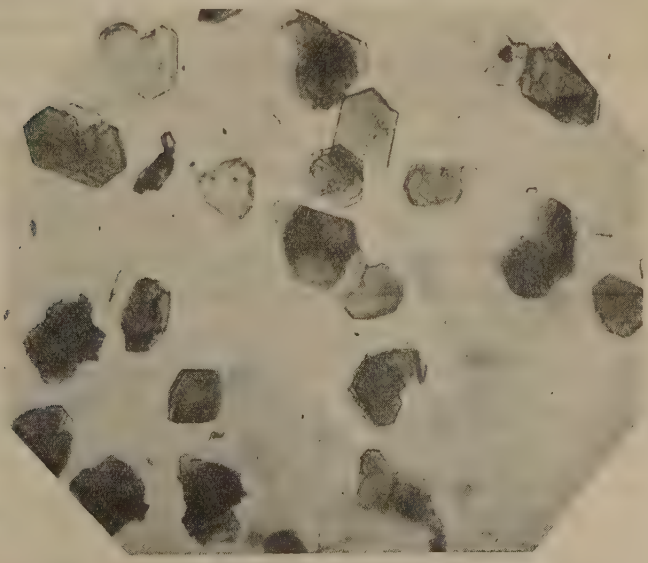

Fig. 1. Chlorite flakes from the Hitachi mine. (×25)

powdery masses in epidote-chlorite-quartz-albite veins in so-called meta-diorite, which is frequently found associating with the ore deposit of this mine, cupriferous pyrite deposits in crystalline schists.

Chemical analysis The microscopic study confirmed that the original specimen is composed of chlorite flakes without impurities. By way of precaution the fine dusty part was removed from the original powder by elutriation, and clear crystal flakes of the chlorite were accumulated, dried, and analysed chemically. Its chemical composition is as follows;

SiO_2 25.76%, Al_2O_3 21.26%, Fe_2O_3 6.75%, FeO 14.60%, CaO 0.90%, MgO 18.64%, $H_2O(-)$ 1.32%, $H_2O(+)$ 10.33%, total 99.56% (analyst, H. Sato).

This chemial composition can give the following structural formula based on the negative charges as 28,

$(Mg_{2\cdot82}\ Ca_{0\cdot09}\ Fe'''_{0\cdot52}\ Fe''_{1\cdot24}\ Al_{1\cdot17})\ (Al_{1\cdot38}\ Si_{2\cdot64})\ O_{10}\ (OH)_8$

X-ray powder diffraction data X-ray powder diffraction data for the specimen analysed chemically were obtained by Philips Geiger counter X-ray diffractometer (Table 1).

Table 1. X-ray powder diffraction data for chlorite from the Hitachi mine, Ibaragi Prefecture. (Cu$K\alpha$ radiation)

hkl	*d*	*I*	*hkl*	*d*	*I*
001	14.7 Å	41		2.151 Å	4
002	7.14	>90	007	2.027	10
003	4.75	57	$13\bar{5}$, 204	2.014	11
004	3.56	>90	135, $20\bar{8}$	1.895	5
005	2.840	23	$13\bar{6}$, 205	1.824	4
	2.652	2		1.762	3
131, $20\bar{2}$	2.600	5	136, $20\bar{7}$	1.713	5
$13\bar{2}$, 201	2.564	6	137, $20\bar{8}$	1.578	8
132, $20\bar{3}$	2.462	6	060, $33\bar{1}$, 331,	1.549	5
$13\bar{3}$, 202	2.398	6		1.514	4
006	2.356	4	00,10	1.425	8
133, $20\bar{4}$	2.238	5	$13\bar{9}$, 208	1.397	8

The (004) spacing was obtained as 3.563 ±0.002 Å by unfiltered Cu radiation using quartz as standard. Referring to this data as well as other (00*l*) spacings, the (001) spacing was obtained as 14.2±0.1 Å.

Differential thermal analysis curve The thermal curve recorded by the mean heating rate of 10°C. per minute is as illustrated in Fig. 2. It has the first endothermic peak between 600° and 700°C., and the second endothermic peak between 700° and 800°C., and an exothermic peak between 800° and 900°C..

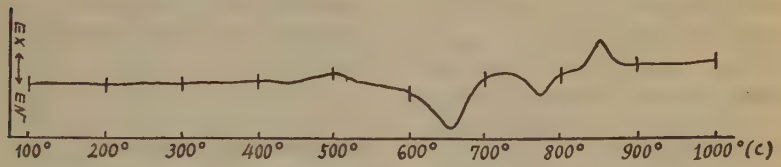

Fig. 2. D. t. a. curve for the chlorite from the Hitachi mine.

Classification The classification of the chlorite minerals has long been discussed from the chemical point of view and recently taking the structural study into consideration. However, we should take our time until we have opportunity for a thorough discussion of nomenclature problems. At present, the possible classification of the chlorite now in question can be given as that it is chemically near to delessite and/or ripidolite, both of which are two principal chlorite species in Fe-Mg chlorites. Its chemical composition can be plotted in the ripidolite area of Hey diagram[1]. Accurate thermal and X-ray data for chlorites grouped as delessite and/or ripidolite are wanting up to date.

Acknowledgement The writers are indebted to T. Takeyasu of the Hitachi Mine for supplying this valuable specimen.

1) M. H. Hey: Miner. Mag., 30, 277 (1955).

Manuscript received March 7, 1956.

INDEX TO VOLUME 1

Aegirine from Hoansan, Korea. (Ito) 252
Alpha radioactivity of the neucleus minerals, and the development of pleochroic haloes (Hayase).....213
Amphibole, parailel intergrowth of pyroxene and, (Sueno) 185
Analcite, dielectric behaviour of apophyllite and, (Kiriyama, Ibamoto, Koizumi, Kitagaki) 313
Andalusite de Koshinmen. (Ito) ...126
Aomine, S. and Higashi, T. Clay minerals of decomposed andesitic agglomeratic lava at Yoake. 278
Apophyllite, dielectric behaviour of analcite and, (Kiriyama, Ibamoto, Koizumi, Kitagaki) 313

Beta-rays, the number of counts of, detected by an end-window Geiger-Mueller counter. (Katayama) 170, 303
Biotite crystals from the Myôgô-hô, Miyagi Prefecture, Japan. (Minato, Takano, Ichimura) 140
Bismuthinite-stibnite series, minerals of, with special reference to Horobetsuite. (Hayase).....189
Boulangerite in sulphide ores from the Obira mine, Kyushu, Japan. (Miyahisa) 323

Cations, effects of constituent, on the refractive indices of orthopyroxenes. (Hori) 359
Cheng Chi Kuo. See Takubo, J. ... 25
Chlorite from the Hitachi mine, Ibaragi Prefecture. (Sato, Sudo) 395
Chlorite, iron-rich, from Shôgasé, Kôchi Prefecture, Japan. (Shirozu) 224
Chlorite, magnesium-rich, from the Wanibuchi mine, Shimane Prefecture. (Sakamoto, Sudo) 348
Clay minerals of decomposed andesitic agglomeratic lava at Yoake. (Aomine, Higashi) 278
Clinoclasite from Kitabira, Yamaguchi Prefecture, Japan. (Minato) 89
Conichalcite from Kitabira, Yamaguchi Prefecture, Japan. (Minato, Takano) 48
Cordierite and indialite, optical properties and unit cell dimensions of, (Iiyama) 372
Crystal structure of orpiment (As_2S_3) refined. (Morimoto) 160

Dehydration curves, and differencial thermal analysis curves of zeolites. (Koizumi) 36
Diadochic substitution in silicates. (Hori).....109
Dielectric behaviour of apophyllite and analcite. (Kiriyama, Ibamoto, Koizumi, Kitagaki).....313
Dielectric constants of minerals. (Takubo, Ukai, Kakitani) 3
Dielectric constants of rocks. (Takubo, Ukai, Cheng) 25
Differential thermal analysis curves and dehydration curves of zeolites. (Koizumi) 36
Doi, K. A new method for estimating the termination effect in Fourier analysis 329

Electrical conduction of pyrite.

(Sasaki) 290
Épidote de Munam. (Ito) 63
Épidote de Takéshi. (Ito) 64

Ferroludwigite from the Kamaishi Iron Mine, Iwate Prefecture. (Watanabe, Ito) 84
Fourier analysis, a new method for estimating the termination effect in, (Doi) 329

Geiger-Mueller counter, the number of counts of beta-rays detected by an end-window, (Katayama) 170, 303

Halloysite, on the thermal transformation of kaolinite and, (Nakahira) 129
Harada, Z. and Hariya, Y. On the thermo-electric potential of pyrite from the Tutiya-Isizaki mine, Hokkaido, Japan 97
Hariya, Y. See Harada, Z. 97
Hayase, I. Uranium contents of zircons in granite 147
The development of pleochroic haloes and the alpha radioactivity of the nucleus minerals ... 213
Hayase, K. Minerals of bismuthinite-stibnite series with special reference to horobetsuite from the Horobetsu mine, Hokkaido, Japan 189
Heikolite, on the anomalous optical properties of, (Shoda) 69
Higashi, T. See Aomine, S. 278
High-temperature optics of natural sodic plagioclases. (Kano) 255
Himeshima, Ooita Prefecture, vivianite from, (Minato, Kinoshita, Okamoto) 337
Hitachi mine, Ibaragi Prefecture, chlorite from, (Sato, Sudo) 395
Hoansan, in the Fukushin-san district, Korea, aegirine from, (Ito) 252
Hol Kol, Suan, North Korea, Suanite, a new magnesium borate mineral from, (Watanabe) 54
Hori, F. On the diadochic substitution in silicates 109
Effects of constituent cations on the refractive indices of orthopyroxenes 359
Horobetsu mine, Hokkaido, horobetsuite from, (Hayase) 189
Horobetsuite from the Horobetsu mine, Hokkaido, minerals of bismuthinite-stibnite series with special reference to, (Hayase) ... 189
Hydrated halloysite, particle shape of a certain clay of, (Sudo) 66

Ibamoto, H. See Kiriyama, R. 313
Ichimura, T. See Minato, H. 140
Iiyama, T. Optical properties and unit cell dimensions of cordierite and indialite 372
Indialite, optical properties and unit cell dimensions of, (Iiyama) 372
Inesite from Rendaiji. (Takasu) ... 242
Ito, J. Épidote de Munam 63
Épidote de Takéshi 64
See Watanabe, T. 84
Andalusite de Koshinmen 126
Riebeckite from Sepori in the Fukushin-san district, Korea. ... 250
Aegirine from Hoansan, in the Fukushin-san district, Korea 252
Iwai, S. On the structural variations of some Japanese kaolinites. 233

Kakitani, S. See Takubo, J. 3
Kamaishi Iron Mine, Iwate Prefecture, paigeite from, (Watanabe, Ito) 84

Kano, H. High-temperature optics of natural sodic plagioclases.....255
Kaolinite, on the structural variations of some Japanese, (Iwai)...233
Kaolinite, on the thermal transformation of, (Nakahira).....129
Katayama, N. The number of counts of beta-rays detected by an end-window Geiger-Mueller counter 170, 303
Kinoshita, K. See Minato, H. 337
Kiriyama, R. with Ibamoto, H., Koizumi, M. and Kitagaki, R. Dielectric behaviour of apophyllite and analcite.....313
Kitabira, Yamaguchi Prefecture, clinoclasite from, (Minato) 89
conichalcite from, (Minato, Takano) 48
Kitagaki, R. See Kiriyama, R. 313
Koizumi, M. The differential thermal analysis curves and the dehydration curves of zeolites 36
See Kiriyama, R. 313
Korekawa, M. See Ueda, T. 198
Koshinmen, andalusite de. (Ito) ...126

Lattice destruction, X-ray measurements of, and its recovery on some radioactive minerals, (Ueda, Korekawa).....198

Minato, H. On clinoclasite from Kitabira, Yamaguchi Prefecture, Japan 89
with Kinoshita, K. and Okamoto, Y. Vivianite from Himeshima, Ooita Prefecture, Japan 337
with Takano, Y. On conichalcite from Kitabira, Yamaguchi prefecture, Japan 48
with Takno, Y. and Ichimura, T. Biotite crystals from the Myôgô-hô, Miyagi Prefecture, Japan.....140
Miyahisa, M. Boulangerite in sulphide ores from the Obira mine, Kyushu, Japan.....323
Morimoto, N. The crystal structure of orpiment (As_2S_3) refined. 160
Munam, épidote de, (Ito) 63
Myôgô-hô, Miyagi Prefecture, biotite crystals from, (Minato, Takano, Ichimura) 140

Nakahira, M. On the thermal transformation of kaolinite and halloysite 129
Nucleus minerals, the alpha radioactivity of, (Hayase) 213

Obira mine, Kyushu, boulangerite from, (Miyahisa) 323
Okamoto, Y. See Minato, H. 337
Optical properties of heikolite, (Shoda) 69
Optical properties and unit cell dimensions of cordierite and indialite. (Iiyama).....372
Orpiment, the crystal structure of, refined, (Morimoto) 160
Orthopyroxenes, effects of constituent cations on the refractive indices of, (Hori) 359

Paigeite (ferroludwigite) from the Kamaishi Iron Mine, Iwate Prefecture, Japan. (Watanabe, Ito)... 84
Parallel intergrowth of pyroxene and amphibole in plutonic rocks. (Sueno) 185
Particle shape of a certain clay of hydrated halloysite, as revealed by the electron microscope. (Sudo) 66
Pleochroic haloes, the development of, (Hayase).....213

Pyrite, on the electrical conduction of, (Sasaki) 290
Pyrite from the Tutiya-Isizaki mine, Hokkaido, on the thermo-electric potential of, (Harada, Hariya) 97
Pyroxene and amphibole in plutonic rocks, parallel intergrowth of, (Sueno) 185

Radioactive minerals, X-ray measurements of the lattice destruction and its recovery, (Ueda, Korekawa) 198
Refractive indices of orthopyroxenes, effects of constituent cations, (Hori).....359
Rendaiji, on inesite from, (Takasu) 242
Riebeckite from Sepori in the Fukushin-san district, Korea. (Ito) 250

Sakamoto, T. and Sudo, T. Magnesium-rich chlorite from the Wanibuchi mine, Shimane Prefecture 348
Sasaki, A. On the elecrical conduction of pyrite 290
Sato, H. and Sudo, T. Chlorite from the Hitachi mine, Ibaragi Prefecture 395
Sepori in the Fukushin-san district, Korea, riebeckite from, (Ito) 250
Shirozu, H. Iron-rich chlorite from Shôgasé, Kôchi Prefecture, Japan 224
Shoda, T. On the anomalous optical properties of Heikolite..... 69
Shôgasé, Kôchi Prefecture, iron-rich chlorite from, (Shirozu) ...224
Silicates, on the diadochic substitution in, (Hori) 109
Sodic plagioclase, high-temperature optics of, (Kano) 255
Structural variations of some Japanese kaolinites. (Iwai) 233
Suanite, a new magnesium borate mineral from Hol Kol, Suan, North Korea. (Watanabe) 54
Sudo, T. Particle shape of a certain clay of hydrated halloysite, as revealed by the electron microscope 66
See Sakamoto, T. 348
See Sato, H. 395
Sueno, T. Parallel intergrowth of pyroxene and amphibole in plutonic rocks 185

Takano, Y. See Minato, H. 48, 140
Takasu, S. On inesite from Rendaiji.....242
Takéshi, épidote de, (Ito) 64
Takubo, J. with Ukai, Y. and Cheng Chi Kuo. On the dielectric constants of rocks 25
with Ukai, Y. and Kakitani, S. On the dielectric constants of minerals..... 3
Termination effect in Fourier analysis, a new method for estimating, (Doi).....329
Thermal transformation of kaolinite and halloysite. (Nakahira). 129
Thermo-electric potential of pyrite from the Tutiya-Isizaki mine, Hokkaido. (Harada, Hariya)..... 97
Tutiya-Isizaki mine, Hokkaido, on the thermo-electric potential of pyrite from, (Harada, Hariya)... 97

Ueda, T. and Korekawa, M. X-ray measurements of the lattice destruction and its recovery on some radioactive minerals.....198
Ukai, Y. See Takubo, J. 3, 25
Unit cell dimensions of cordierite

and indialite, (Iiyama) 372
Uranium contents of zircons in granite. (Hayase) 147

Vivianite from Himeshima, Ooita Prefecture, Japan. (Minato, Kinoshita, Okamoto) 337

Wanibuchi mine, Shimane Prefecture, magnesium-rich chlorite from, (Sakamoto, Sudo) 348
Watanabe, T. Suanite, a new magnesium borate mineral from Hol Kol, Suan, North Korea 54
with Ito, J. Paigeite (ferroludwigite) from the Kamaishi Iron Mine, Iwate Prefecture, Japan ... 84

Yoake, clay minerals of decomposed andesitic agglomeratic lava at, (Aomine, Higashi) 278

Zeolites, the differential thermal analysis curves and the dehydration curves of (Koizumi) 36
Zircons in granite, uranium contents of, (Hayase).....147

Contents of "KOBUTSUGAKU ZASSHI,"

Journal of the Mineralogical Society of Japan

in Japanese

VOL. 2, No. 5 (January, 1956)

Original Articles

Manganiferous Epidote from the Kakinomoto Mine, Kôchi Prefecture ... F. Hirowatari...331

Hydrothermal Reaction of Dehydrated Laumontite ... R. Kiriyama, M. Koizumi, K. Yamada and R. Kitagaki...347

Hydrothermal Reaction of Dehydrated Heulandite ... R. Kiriyama, M. Koizumi, K. Yamada and R. Kitagaki...359

A Clay Mineral Accompanied by Epithermal Iron Sulphide Deposits ... K. Kinoshita and S. Tanaka...367

Studies on the Chemical Analyses of Several Ores with Regard to Their Mineral Composition (Part 3), Chrome Ore ... T. Imai and H. Nagashima...375

Short Communications

Gibbsite in "Nishime-clay" from Yuri-Gun, Akita Prefecture ... S. Honda...386

Calcite from the Yanahara Mine, Okayama Prefecture ... H. Takeda...393

Infrared Absorption Studies on Some Clay Minerals ... S. Kakitani...398

Gersdorffite of the Okura Mine, Niigata Prefecture ... H. Gohara...403

Communications on Minerals of Japan (Part 8) ... Mumeikai Group...407

20. Pyroxmangite from Kamiotomo, Iwate Prefecture ... K. Sakurai, K. Nagashima and S. Takasu

Reviews

The Fourth Clay Minerals Conference ... T. Sudo...413

Proceedings ... 429

Contents of "KOBUTSUGAKU ZASSHI,"

Journal of the Mineralogical Society of Japan

in Japanese

Vol. 2, No. 6 (May, 1956)

Original Articles

Mineralogical Study of Manganese Dioxide Mineral (Part 1) ..... Y. Ukai, S. Nishimura and T. Maeda...431

Some Tellurium Minerals from the Kobetsuzawa Mine, Sapporo, Hokkaido .....M. Ishibashi...447

Studies on the Chemical Analyses of Several Ores with Regard to Their Mineral Composition (Part 4) Rare Earths Ore ..... T. Imai and T. Asada...458

Hydrothermal Reaction of Dehydrated Analcite..... R. Kiriyama, M. Koizumi, K. Yamada and R. Kitagaki...464

Short Communications

Fayalite from Ôsunaba, Okayama City .....H. Takeda and Y. Satô...471

Communications on Minerals of Japan (Part 9) .....Mumeikai Group...474

21. Clinozoisite from Arai, Saitama Prefecture..... K. Sakurai and K. Nagashima.

Reviews

Analytical Methods of Uranium and Thorium in Ores and Minerals ... Y. Ukai and S. Nishimura...477

Proceedings 501

Index to Volume 2.....502

Printed by "HERALD" Printing Co, Ltd.